A New Test of Dynamical Dark Energy Models and Cosmic Tensions in Hořava Gravity

Eleonora Di Valentino, Nils A. Nilsson, Mu-In Park

Monthly Notices of the ROYAL ASTRONOMICAL SOCIETY

MNRAS **519,** 5043–5058 (2023) https://doi.org/10.1093/mnras/stac3824
Advance Access publication 2023 January 3

A new test of dynamical dark energy models and cosmic tensions in Hořava gravity

Eleonora Di Valentino [1], Nils A. Nilsson[2,3] and Mu-In Park [3]★

[1] *School of Mathematics and Statistics, University of Sheffield, Hounsfield Road, Sheffield S3 7RH, UK*
[2] *SYRTE, Observatoire de Paris-PSL, Sorbonne Université, CNRS UMR8630, LNE, 61 avenue de l'Observatoire, F-75014 Paris, France*
[3] *Center for Quantum Spacetime (CQUeST), Sogang University, Seoul 121-742, South Korea*

Accepted 2022 December 30. Received 2022 December 27; in original form 2022 November 25

ABSTRACT

Hořava gravity has been proposed as a renormalizable, higher derivative, Lorentz-violating quantum gravity model without ghost problems. A Hořava gravity-based dark energy (HDE) model for dynamical dark energy has also been proposed earlier by identifying all the extra (gravitational) contributions from the Lorentz-violating terms as an *effective* energy–momentum tensor in Einstein equation. We consider a complete cosmic microwave background, baryon acoustic oscillation (BAO), and supernova Ia data test of the HDE model by considering general perturbations over the background perfect HDE fluid. Except from BAO, we obtain the preference of *non-flat* universes for all other data set combinations. We obtain a positive result on the cosmic tensions between the Hubble constant H_0 and the cosmic shear S_8, because we have a shift of H_0 towards a higher value, though not enough for resolving the H_0 tension, but the value of S_8 is unaltered. This is in contrast to a rather decreasing H_0 but increasing S_8 in a non-flat Lambda cold dark matter (LCDM). For all other parameters, like $\Omega_{\rm m}$ and Ω_Λ, we obtain quite comparable results with those of LCDM for all data sets, especially with BAO, so that our results are close to a *cosmic concordance* between the data sets, contrary to the standard non-flat LCDM. We also obtain some undesirable features, like an almost *null* result on Ω_k, which gives back the flat LCDM, if we do not predetermine the sign of Ω_k, but we propose several promising ways for improvements by generalizing our analysis.

Key words: cosmic background radiation – cosmological parameters – dark energy – cosmology: theory.

1 INTRODUCTION

In 2009, Hořava proposed a renormalizable, higher derivative, Lorentz-violating quantum gravity model without the ghost problem, due to anisotropic scaling dimensions for space and time *à la* Lifshitz and DeWitt (Lifshitz 1941; DeWitt 1967; Horava 2009). In the last 12 yr, there have been a lot of work on its various aspects [see Wang (2017) for a brief review and extensive literature]. In particular, Park (2009) interpreted the *dark energy* as an *effective* energy–momentum in Einstein equation due to the extra contributions from the Lorentz-violating terms.

The Hořava gravity-based dark energy (HDE) model explains naturally the non-interacting nature of the dark energy sector, except the gravitational interactions since it was originally a part of the gravity sector, with the ordinary matter sector. Furthermore, it also predicts *dynamical* dark energy behaviour in the cosmic evolution, depending on the purported Hořava gravity action, which may contain various spatially higher derivative ultraviolet (UV) Lorentz-violating terms [up to sixth order or $z = 3$ in $(3 + 1)$ dimensions for renormalizability (Horava 2009)] and infrared (IR) Lorentz-violating terms. A peculiar property of HDE is that a spatially non-flat universe may be more 'natural' due to genuine contributions from higher spatial derivatives (Park 2009) since, for a spatially flat universe, the usual Friedmann–Lemaitre–Robertson–Walker (FLRW) *background* cosmology (Friedman 1922; Lemaitre 1927) is the same as in general relativity (GR). In other words, Hořava gravity can be a 'natural laboratory' for the test of a non-flat universe in the standard Lambda cold dark matter (LCDM) cosmology.

On the other hand, with the increased precision of cosmological data, some cosmic tensions between different data sets are becoming clearer (Di Valentino et al. 2021b, c; Shah, Lemos & Lahav 2021; Abdalla et al. 2022) within the standard LCDM paradigm and its complete resolution is a challenging problem in current cosmology. In particular, there have been various proposals (Knox & Millea 2020; Di Valentino et al. 2021a; Jedamzik, Pogosian & Zhao 2021; Kamionkowski & Riess 2022; Perivolaropoulos & Skara 2022) trying to address the tensions involving the Hubble constant H_0 (Verde, Treu & Riess 2019; Riess et al. 2022) and $S_8 \equiv \sigma_8\sqrt{\Omega_m/0.3}$, measured by cosmic shear experiments (Asgari et al. 2021; Abbott et al. 2022b), between cosmic microwave background (CMB) data and local measurements at lower redshifts, which corresponds to the *mismatches between the early and late universe*, but a resolution at the fundamental level is still missing. Moreover, when the possibility of a *closed* universe is considered (Di Valentino, Melchiorri & Silk 2019; Di Valentino et al. 2021d, f; Handley 2021; Semenaite et al. 2022; Yang et al. 2022), the tensions become worse, due to a decreasing H_0 but increasing S_8, and a new problem appears, called the *discordance* problem, which means 'the lack of *concordance* – in other words, the lack of consistency – with other observations'; for example, the closed universe preferred by Planck predicts $\Omega_{\rm m} \sim 0.5$ and consequently $\Omega_\Lambda \sim 0.5$, in sharp contrast to the conventional

★ E-mail: muinpark@gmail.com

value $\Omega_m \sim 0.3$ and $\Omega_\Lambda \sim 0.7$ for the local measurements or flat LCDM.

This motivated Nilsson & Park (2022) to analyse current cosmological data, including baryon acoustic oscillations (BAOs), for the standard (background) FLRW cosmology with the HDE model and they found some improvements of the Hubble constant tension with a preference of a 'closed' universe but *without* the problems of too large Ω_m and too small Ω_Λ in a non-flat LCDM, i.e. improving the discordance problem. However, the previous analysis was not complete in two aspects. First, due to the lack of *perturbations* of matter and dark energy, one cannot spell out the S_8 tension from the amplitude σ_8 of matter density fluctuations on scales of 8 Mpc h^{-1}. Secondly, due to the *algorithmic* limitation of the Metropolis–Hastings algorithm (Robert 2015), the convergent χ^2 statistics for separate data sets was not possible. From this second limitation, Ω_m and Ω_Λ were obtained only for *all* the data sets whose reasonable value seems to support the lack of the discordance problem for *separate* data sets, but its explicit confirmation in each data set is still absent.

In this paper, in order to fill the gap, we extend the background analysis by considering *dark-energy perturbations* and using the full CMB data via CAMB/COSMOMC. In Section 2, we consider the theoretical set-up for the cosmological perturbations of the HDE model on a *non-flat* FLRW background, based on the fluid approach for the perturbed HDE. We compare our HDE model whose equation of state (EoS) parameter is rapidly varying or fluctuating with the standard CPL model and show a good agreement in the comoving angular diameter distance, which supports the robustness of our HDE model in analysing observational data. We also present the implicit assumptions in our fluid approach and initial conditions for solving perturbation equations. In Section 3, we describe our methodology for the analysis and the data sets under consideration. In Section 4, we present and discuss our obtained results. In Section 5, we conclude by proposing several promising directions to improve our analysis.

2 THEORETICAL SET-UP

2.1 Dynamical dark energy model in Hořava gravity: HDE model

We start by briefly reviewing the dynamical dark energy model in Hořava gravity, named HDE model (Park 2009). To this end, we consider the Arnowitt–Deser–Misner (ADM; Arnowitt, Deser & Misner 2008) metric

$$ds^2 = -N^2c^2dt^2 + g_{ij}(dx^i + N^i dt)(dx^j + N^j dt) \tag{1}$$

and the (non-projectable[1]) Hořava gravity action *à la* Lifshitz and DeWitt (HLD; Lifshitz 1941; DeWitt 1967; Horava 2009; Shin & Park 2017), given by

$$S_{\rm HLD} = \int dt d^3x \sqrt{g} N \left[\frac{2}{\kappa^2}(K_{ij}K^{ij} - \lambda K^2) - \mathcal{V} \right], \tag{2}$$

$$-\mathcal{V} = \sigma + \xi R + \alpha_1 R^2 + \alpha_2 R_{ij}R^{ij} + \alpha_3 \frac{\epsilon^{ijk}}{\sqrt{g}} R_{il}\nabla_j R^l{}_k + \alpha_4 \nabla_i R_{jk}\nabla^i R^{jk} + \alpha_5 \nabla_i R_{jk}\nabla^j R^{ik} + \alpha_6 \nabla_i R \nabla^i R, \tag{3}$$

which is power-counting renormalizable without the ghost problem in physical TT (transverse-traceless) graviton modes. Here,

$$K_{ij} = \frac{1}{2N}(\dot{g}_{ij} - \nabla_i N_j - \nabla_j N_i) \tag{4}$$

is the extrinsic curvature [the dot ($\dot{}$) denotes the time derivative with respect to physical time t], ∇_i is the covariant derivative with respect to 3-metric g_{ij}, R_{ij} is the Ricci tensor of a 3-geometry, $K = g_{ij}K^{ij}$ and $R = g_{ij}R^{ij}$ are their traces, ϵ^{ijk} is the Levi–Civita symbol, and κ, λ, ξ, α_i, and σ are coupling constants.

From the detailed balance condition (DBC), which was adopted from quantum critical phenomena in condensed matter systems (Horava 2009), the number of independent coupling constants reduces to six, i.e. κ, λ, μ, ν, Λ_W, and ω for a viable gravity theory in the IR (Kehagias & Sfetsos 2009; Park 2009), and the theory parameters are given by

$$\sigma = \frac{3\kappa^2\mu^2\Lambda_W^2}{8(3\lambda-1)},\ \xi = \frac{\kappa^2\mu^2(\omega-\Lambda_W)}{8(3\lambda-1)},\ \alpha_1 = \frac{\kappa^2\mu^2(4\lambda-1)}{32(3\lambda-1)},$$
$$\alpha_2 = -\frac{\kappa^2\mu^2}{8}\alpha_3 = \frac{\kappa^2\mu}{2\nu^2},\ \alpha_4 = -\frac{\kappa^2}{82\nu^4} = -\alpha_5 = -8\alpha_6, \tag{5}$$

with $\mu^2 > 0$ (<0) for a positive (negative) cosmological constant ($\sim\Lambda_W$). Here, DeWitt's IR Lorentz violation parameter λ (DeWitt 1967) can be arbitrary, but below we will restrict to the case $\lambda = 1$ so that our analysis agrees with the standard analysis in GR at low energies. The UV couplings $\alpha_3, ..., \alpha_6$ do not appear explicitly in our analysis below, but we will discuss their interesting role in the dark energy perturbations in Section 5.

Then, we may consider the gravity equations of motion for our universe with matter (ordinary and dark matter, and radiation) as

$$G^{\mu\nu} = \frac{8\pi G}{c^4}\left(T^{\mu\nu}_{\rm matter} + T^{\mu\nu}_{\rm DE}\right) \tag{6}$$

for the Einstein tensor $G^{\mu\nu} = \hat{R}^{\mu\nu} - (1/2)\hat{g}^{\mu\nu}\hat{R}$ with the $(3+1)$-dimensional Ricci tensor $\hat{R}^{\mu\nu}$, Ricci scalar $\hat{R}$, and covariant derivative $\hat{\nabla}_\mu$ by treating all the Lorentz-violating contributions from the HLD action (equation 2) as an 'effective' dark energy *fluid* with the energy–momentum tensor $T^{\mu\nu}_{\rm DE}$, including the cosmological constant term (Park 2009). This interpretation is based on the fact that the dark energy is defined by the 'unknown' contributions, other than dark matter, in our universe when described by GR. An important direct consequence of the interpretation is the (usually assumed) *non-interacting* nature of dark energy, except the gravitational interactions, with matter can be easily explained.[2] Moreover, from the Bianchi identity $\hat{\nabla}_\mu G^{\mu\nu} = 0$ and the covariant conservation law

[1] In the *projectable* case (Horava 2009; Mukohyama 2009), where the lapse function N is a function of time only, there exists one extra scalar graviton mode. But in this paper, we will not consider those cases in order to recover GR at the low-energy (or IR) limit, not to mention its pathological ghost behaviour (Bogdanos & Saridakis 2010; Koyama & Arroja 2010; Cerioni & Brandenberger 2011) that is though somewhat improved in the extended model with the dynamical lapse function (Blas, Pujolas & Sibiryakov 2010). Even in the *non-projectable* case, where N is a function of space as well as time generally, it has also been known to have similar problems (Blas, Pujolas & Sibiryakov 2009) that have been the motivation for the extended model in Blas et al. (2010), but it has been later found that there is no extra graviton mode problem in cosmological perturbations at the linear order (Gao et al. 2010; Shin & Park 2017).

[2] If there is a way to identify the dark matter as well as the dark energy from the gravity sector, one can also explain the non-interaction of dark matter with ordinary matter and radiation but with a possible interaction of dark energy and dark matter (Gavela et al. 2009). In *projectable* Hořava gravity, CDM can be naturally introduced as an 'integration constant' (Mukohyama 2009). If one can realize the similar CDM behaviour in its non-projectable version with 'a_i-extended terms' (Blas et al. 2010), which is related to *Einstein aether* (Jacobson & Mattingly 2004) or *Standard-Model-Extension* (SME) gravity at low energy (O'Neal-Ault, Bailey & Nilsson 2021), one can explain

of matter $\hat{\nabla}_\mu T^{\mu\nu}_{\rm matter} = 0$, one can find the conservation of dark energy $\hat{\nabla}_\mu T^{\mu\nu}_{\rm DE} = 0$ as well, even with the Lorentz-violating terms of the HLD action (equation 2).[3]

As a background cosmology metric, we consider the homogeneous and isotropic FLRW metric (Friedman 1922; Lemaitre 1927)

$$ds^2 = -c^2dt^2 + a^2(t)\left[\frac{dr^2}{1-\mathcal{K}r^2/R_0^2} + r^2(d\theta^2 + \sin^2\theta d\phi^2)\right] \quad (7)$$

with the (spatial) curvature parameter $\mathcal{K} = +1, 0, -1$ for a closed, flat, open universe, respectively, and the current curvature radius R_0 at $a(t_0) \equiv 1$. Assuming the perfect fluid form of matter (background) energy–momentum tensor $\bar{T}^\mu_\nu = \mathrm{diag}(-\rho, p, p, p)$ with energy density ρ and pressure p, we obtain the Friedmann equations as

$$\left(\frac{\dot{a}}{a}\right)^2 = \frac{8\pi G}{3c^2}(\rho_{\rm matter} + \rho_{\rm DE}) - \frac{c^2\mathcal{K}}{R_0^2a^2}, \quad (8)$$

$$\frac{\ddot{a}}{a} = -\frac{4\pi G}{3c^2}[(\rho_{\rm matter} + \rho_{\rm DE}) + 3(p_{\rm matter} + p_{\rm DE})], \quad (9)$$

where we introduce the energy density and pressure for the dark energy (HDE)[4] as

$$\rho_{\rm DE} = \frac{3\kappa^2\mu^2}{8(3\lambda-1)}\left(\frac{\mathcal{K}^2}{R_0^4a^4} + \frac{2\omega\mathcal{K}}{R_0^2a^2} + \Lambda_W^2\right), \quad (10)$$

$$p_{\rm DE} = \frac{\kappa^2\mu^2}{8(3\lambda-1)}\left(\frac{\mathcal{K}^2}{R_0^4a^4} - \frac{2\omega\mathcal{K}}{R_0^2a^2} - 3\Lambda_W^2\right), \quad (11)$$

respectively, by defining the fundamental constants in GR, i.e. speed of light c, Newton's constant G, and cosmological constant Λ as (we have set $\lambda = 1$)[5]

$$c^2 = \frac{\kappa^4\mu^2\Lambda_W}{32}, \; G = \frac{\kappa^2c^2}{32\pi}, \; \Lambda = \frac{3}{2}\Lambda_W c^2. \quad (12)$$

Note that, for the spatially flat universe with $\mathcal{K} = 0$, all the contributions from the higher derivative terms disappear and we recover the same background cosmology as in GR, which means a return to the flat LCDM model. On the other hand, it is important to note that the energy-momentum tensor of dark energy has the perfect fluid form[6]

$$\bar{T}^\mu_{\nu\,\rm DE} = \mathrm{diag}(-\rho_{\rm DE}, p_{\rm DE}, p_{\rm DE}, p_{\rm DE}) \quad (13)$$

and satisfies the covariant conservation law

$$\bar{\nabla}_\mu \bar{T}^{\mu\nu}_{\rm DE} = \dot{\rho}_{\rm DE} + 3H(\rho_{\rm DE} + p_{\rm DE}) = 0 \quad (14)$$

with the Hubble parameter $H(t) \equiv \dot{a}/a$, consistently with (6), where $\bar{\nabla}_\mu$ denotes the covariant derivative with respect to the background metric (7).

the null result in direct detection of dark matter via particle interactions [see Section 5, list (ii), for further discussions].

[3]One may say that HLD action (2) can couple only to the covariantly conserved matters $\hat{\nabla}_\mu T^{\mu\nu}_{\rm matter} = 0$, when they are minimally coupled to gravity, since one can find $\hat{\nabla}_\mu T^{\mu\nu}_{\rm DE} = 0$, independently of the matter sector (Devecioglu & Park 2021).

[4]We follow the physical convention of Ryden (Ryden 1970; Park 2009) that disagrees with Horava (2009); $G_{\rm Here} = G_{\rm Horava}/c^2$ and $\Lambda_{\rm Here} = \Lambda_{\rm Horava}c^2$.

[5]If we consider an arbitrary $\lambda \neq 1$, $\rho_{\rm DE}$ also has a $(\dot{a}/a)^2$ term proportional to $(\lambda - 1)$, but its effect is just to shift the overall factors in equations (10) and (11), which corresponds to the shifts in the fundamental constraints c, G, and Λ (Park 2009) [see Section 5, list (iv), for further discussions]. Moreover, there are some additional ambiguities in defining $\rho_{\rm DE}$ and $p_{\rm DE}$, depending on the definitions of c (Kehagias & Sfetsos 2009; Argüelles, Grandi & Park 2015). However, we have found not much difference in the main results for the background analysis (Nilsson & Park, unpublished).

[6]This is essentially due to the property of background FLRW metric. If we consider a spatially anisotropic (Bianchi) universe, we will have anisotropic pressures.

The EoS parameter is given by

$$w_{\rm DE} = \frac{p_{\rm DE}}{\rho_{\rm DE}} = \left(\frac{\mathcal{K}^2 - 2\bar{\omega}\mathcal{K}a^2 - 3\bar{\Lambda}_W^2a^4}{3\mathcal{K}^2 + 6\bar{\omega}\mathcal{K}a^2 + 3\bar{\Lambda}_W^2a^4}\right), \quad (15)$$

where we introduce $\bar{\omega} \equiv \omega R_0^2$, $\bar{\Lambda}_W = \Lambda_W R_0^2$ for convenience. For a flat universe, $\mathcal{K} = 0$, we have $w_{\rm DE} = -1$, which just corresponds to the cosmological constant. However, for any non-flat universe, EoS interpolates from $w_{\rm DE} = 1/3$ (i.e., radiation-like) in the UV limit ($a = 0$) to $w_{\rm DE} = -1$ in the IR limit ($a = \infty$), but other detailed evolution depends on the parameters $\bar{\omega}, \mathcal{K}, \bar{\Lambda}_W$ (Fig. 1). In other words, 'any deviation from the cosmological constant case, $w_{\rm DE} = -1$, in the observational data (see Abbott et al. 2022a for a recent result), is an indication of a non-flat universe in our context'. In this sense, Hořava gravity can be a 'natural laboratory' to test a non-flat cosmology. However, we remark that the observation of $w_{\rm DE}$ only or its derived quantities cannot uniquely determine the theory parameters $\bar{\omega}, \mathcal{K}$ due to a degeneracy between $(\bar{\omega}, \mathcal{K}) \leftrightarrow (-\bar{\omega}, -\mathcal{K})$ in equation (15) (Park 2009).

2.2 Cosmological perturbations on a non-flat background

We consider the perturbed metric as

$$\begin{aligned} N &= a(\eta)[1 + \mathcal{A}(\eta, \boldsymbol{x})], \\ N_i &= a^2(\eta)\mathcal{B}_i(\eta, \boldsymbol{x}), \\ g_{ij} &= a^2(\eta)[\gamma_{ij} + h_{ij}(\eta, \boldsymbol{x})], \end{aligned} \quad (16)$$

where η is the conformal time, defined by $d\eta = dt/a$, and γ_{ij} is the metric for a non-flat three-sphere, $\gamma_{ij} = (1 + \bar{\mathcal{K}}r^2/4)^{-2}\delta_{ij}$, by which the Latin indices $(i, j, \cdots)$ are raised with $\bar{\mathcal{K}} \equiv \mathcal{K}/R_0^2$.

Following the usual scalar–vector–tensor decomposition, we also consider

$$\begin{aligned} \mathcal{B}_i &= D_i\mathcal{B} + S_i, \\ h_{ij} &= 2\mathcal{R}\gamma_{ij} + D_iD_j\mathcal{E} + D_{(i}F_{j)} + H_{ij}, \end{aligned} \quad (17)$$

where D_i is the covariant derivative with respect to γ_{ij}, and S_i, F_i, H_{ij} are transverse vectors and transverse-traceless tensor, respectively, i.e.

$$D_iS^i = D_iF^i = H^i_i = D_iH^i_j = 0. \quad (18)$$

Here, we note that the background FLRW metric is the *projectable* form, i.e. $N = N(\eta)$ (Horava 2009), but the perturbed metric is *non-projectable* with an arbitrary space and time dependence, $N = N(\eta, \boldsymbol{x})$, generally, so that one can obtain the *local* Hamiltonian constraint by varying $N = N(\eta, \boldsymbol{x})$ (Park 2011; Shin & Park 2017). This is a crucial difference from the projectable model (Horava 2009; Mukohyama 2009), where just the *global* Hamiltonian constraint exists so that there is an immovable gap between projectable model and GR, having the local Hamiltonian constraint, and that is the origin of their possessing extra graviton mode.[7]

[7]Of course, the local Hamiltonian constraint does not mean the symmetry generator as in GR. Actually, it is the *second-class* constraint at the fully non-linear level for either the standard non-projectable HLD action (2) (Devecioglu & Park 2021) or the a_i-extended non-projectable model (Bellorin & Restuccia 2011) and there are more (the second-class and the first-class) constraints than GR. However, it is important to note that, in contrast to the a_i-extended model, there is a case (called Case A) where the physical degree of freedom is the same as in GR, even at the fully non-linear level for the non-projectable HLD model. It is still an open problem whether our cosmology corresponds to that case or not.

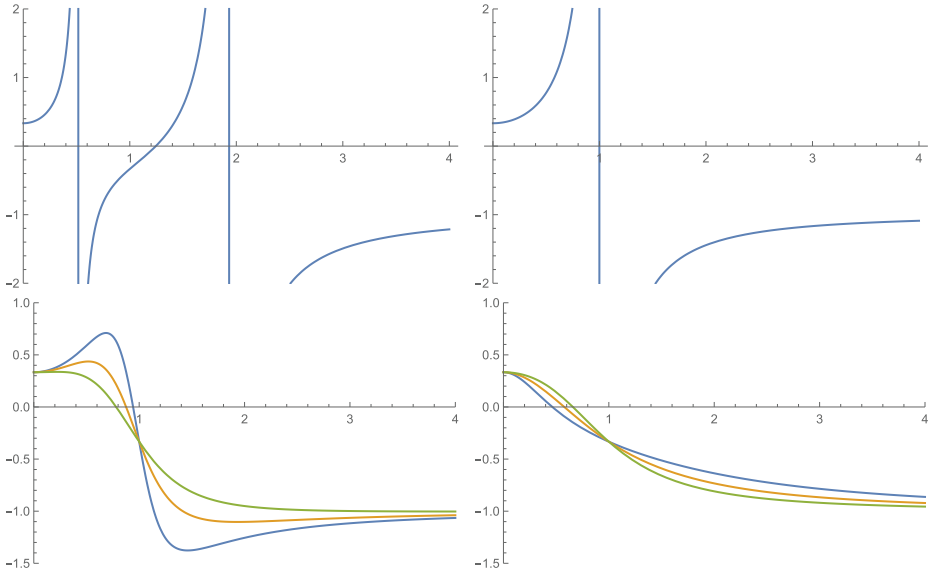

Figure 1. Plots of $w_{\rm DE}$ versus $a(t)$ for (a) $\bar{\omega}^2 > \bar{\Lambda}_W^2,\ \bar{\omega}\mathcal{K} < 0$ (top left), (b) $\bar{\omega}^2 = \bar{\Lambda}_W^2,\ \bar{\omega}\mathcal{K} < 0$ (top right), (c) $\bar{\omega}^2 < \bar{\Lambda}_W^2,\ \bar{\omega}\mathcal{K} < 0$ (bottom left), and (d) $\bar{\omega}^2 < \bar{\Lambda}_W^2,\ \bar{\omega}\mathcal{K} > 0$ (bottom right). Here, we consider $\bar{\omega} = -2$ (top left), $\bar{\omega} = -1$ (top right), $\bar{\omega} = -1/1.3, -1/2, -1/10$ (bottom left), and $\bar{\omega} = 2, 1, 1/2$ (bottom right) with $\mathcal{K} = +1$ (closed universe). Note that there is a degeneracy between $(\bar{\omega}, \mathcal{K}) \leftrightarrow (-\bar{\omega}, -\mathcal{K})$ in $w_{\rm DE}$ of equation (15).

Now, let us consider a perfect fluid of density ρ and pressure p with the energy–momentum tensor

$$T_{\mu\nu} = (\rho + p)u_\mu u_\nu + p g_{\mu\nu} \tag{19}$$

with the four velocity of a comoving observer, $u_\mu u^\mu = -1$, as in the matter and dark energy (13) for the background cosmology. The general form of the perturbed energy-momentum tensor at the linear order can be written (Kodama & Sasaki 1984; Peter & Uzan 2013),

$$\begin{aligned}\delta T_{\mu\nu} = {} & (\delta\rho + \delta p)u_\mu u_\nu + \delta p g_{\mu\nu} + 2(\rho + p)u_{(\mu}\delta u_{\nu)} \\ & + p\delta g_{\mu\nu} + a^2\Sigma_{\mu\nu},\end{aligned} \tag{20}$$

where non-perturbed quantities u_μ, $g_{\mu\nu}$, p, ρ denote the background objects, $\delta u^\mu = a^{-1}(-\mathcal{A}, v^i)$, and $\Sigma_{\mu\nu}$ is the anisotropic stress tensor that represents a non-perfect fluid perturbation, $\Sigma_{ij} = T_{ij} - (1/3)T^k{}_k\gamma_{ij}$, $\Sigma^i{}_i = \Sigma_{0\mu} = 0$, absorbing its trace by the pressure p.

In component form, the perturbations read

$$\begin{aligned}\delta T_{00} &= a^2\rho(\delta_\rho + 2\mathcal{A}), \\ \delta T_{0i} &= -a^2(\rho + p)(v_i + \mathcal{B}_i), \\ \delta T_{ij} &= a^2(p h_{ij} + \gamma_{ij}\delta p + \Sigma_{ij}),\end{aligned} \tag{21}$$

where $\delta_\rho \equiv \delta\rho/\rho$ is the density contrast.

In the cosmological perturbation analysis, a proper choice of gauge is useful, depending on the situation being studied. In Hořava gravity, the 'apparent' action symmetry is the 'foliation-preserving' Diff symmetry (Diff$_\mathcal{F}$) under the coordinate transformation $\delta\eta = -f(\eta)$, $\delta x^i = -\xi^i(\eta, \boldsymbol{x})$, and hence not all the gauges in GR may be allowed. In this paper, we consider the synchronous gauge, which is one of the allowed gauges in Hořava gravity, where we set $\mathcal{A} = \mathcal{B}_i = 0$, since $\mathcal{A}$ and $\mathcal{B}_i$ are the Lagrange multipliers and can be integrated out in the Hamiltonian-reduction (or Faddeev–Jackiw) method (Shin & Park 2017). Actually, in Hořava gravity, this is a natural gauge without much loss of generality of Diff$_\mathcal{F}$, since the residual symmetry of the synchronous gauge corresponds to a Diff$_\mathcal{F}$ with $\delta\eta = -f(\eta)$, $\delta x^i = -\xi^i(\boldsymbol{x})$.

In the synchronous gauge, the equations for the perturbed fluid are given by the perturbed conservation equations, $\delta\hat{\nabla}_\mu T^\mu{}_\nu = 0$ (in momentum space) (Kodama & Sasaki 1984; Ma & Bertschinger 1995; Hu 1998),

$$\delta_\rho{}' = -3\mathcal{H}\left(\frac{\delta p}{\delta\rho} - w\right)\delta_\rho - (1 + w)\left(\theta + \frac{h'}{2}\right), \tag{22}$$

$$\theta' = -\mathcal{H}(1 - 3w)\theta - \frac{w'}{1 + w}\theta + \frac{\delta p/\delta\rho}{1 + w}k^2\delta_\rho - k^2\sigma, \tag{23}$$

where the prime ($'$) denotes the derivative with respect to conformal time η, $\mathcal{H} \equiv (a'/a)$, $\theta \equiv ik^i v_i$, $h \equiv h^i{}_i$, $\equiv -(\hat{k}_i\hat{k}_j - \delta_{ij}/3)\Sigma^i{}_j/(\rho + p)$, and k^i is the comoving wavevector in a *non-flat space* generally, defined by

$$D^i A_{jk\cdots} = ik^i A_{jk\cdots},\ \ D^i D_i A_{jk\cdots} = -k^2 A_{jk\cdots} \tag{24}$$

with $k^2 \geq |\bar{\mathcal{K}}|$ for $\bar{\mathcal{K}} \leq 0$, or $k^2 = l(l + 4)\bar{\mathcal{K}}$ $(l = 0, 1, 2, \cdots)$ for $\bar{\mathcal{K}} > 0$ with the appropriate eigenfunctions (harmonics) $A_{jk\cdots}$ (Vilenkin & Smorodinskii 1964; Hu et al. 1998).

In terms of the gauge invariant, i.e. physical, sound speed $\hat{c}_s$ in the rest frame (Bardeen 1980; Kodama & Sasaki 1984; Hu 1998),

$$\frac{\delta p}{\delta\rho} = \hat{c}_s^2 + \left[3\mathcal{H}\left(\hat{c}_s^2 - w\right) + w'\right]\frac{\rho}{\delta\rho}\frac{\theta}{k^2}, \tag{25}$$

the perturbation equations (22) and (23) reduce to

$$\begin{aligned}\delta_\rho{}' = {} & -3\mathcal{H}\left(\hat{c}_s^2 - w\right)\delta_\rho + 3\mathcal{H}\left[3\mathcal{H}(1 + w)\left(\hat{c}_s^2 - w\right) + w'\right]\frac{\theta}{k^2} \\ & - (1 + w)\left(\theta + \frac{h'}{2}\right),\end{aligned} \tag{26}$$

$$\theta' = -\mathcal{H}\left(1 - 3\hat{c}_s^2\right)\theta + \frac{\hat{c}_s^2}{1 + w}k^2\delta_\rho - k^2\sigma, \tag{27}$$

where we have used the definition of the 'adiabatic' sound speed,

$$c_a^2 \equiv \frac{p'}{\rho'} = w - \frac{w'}{3\mathcal{H}(1 + w)} \tag{28}$$

for the *adiabatic* perturbations, $\delta_a p \equiv c_a^2\delta_a\rho$. Here, note that the adiabatic sound speed $c_{\rm a}$ is determined by the background quantities only and can be infinite at $w = -1$, i.e. cosmological constant, unless $w' = 0$, or even negative depending on w: it just represents $\rho' = 0$ for the former, or even $\rho' < 0$ for the latter while $p' > 0$ (or vice versa).

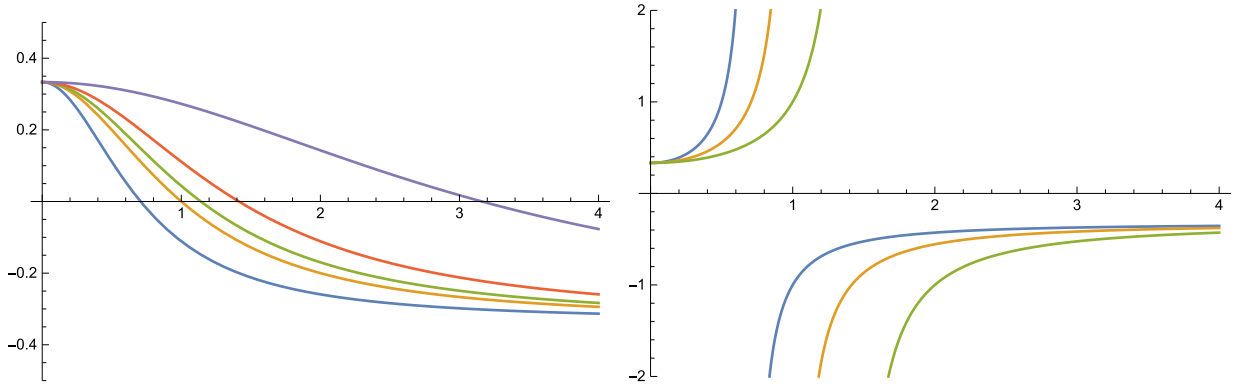

Figure 2. Plots of c_a^2 versus $a(t)$ for $\bar{\omega}\mathcal{K} < 0$ (left) and $\bar{\omega}\mathcal{K} > 0$ (right). Here, we consider the same values of parameters as in Fig. 1: $\bar{\omega} = -2, -1, -1/1.3, -1/2, -1/10$ (left, bottom to top) correspond to the first three cases in Fig. 1, whereas $\bar{\omega} = 2, 1, 1/2$ (right, top to bottom) correspond to the last case in Fig. 1, with $\mathcal{K} = +1$ (or $\bar{\omega} \to -\bar{\omega}$ with $\mathcal{K} = -1$). Note that c_a^2 evolves from $c_a^2 = 1/3$ in the UV limit to $c_a^2 = -1/3$ in the IR limit, but other intermediate details depend on $\bar{\omega}$ and $\mathcal{K}$.

So far, we have not specified any particular fluid and the equations are valid for any 'uncoupled' fluid. Now, by introducing dust matter [non-relativistic baryonic matter and (non-baryonic) CDM with $p_m = 0$] and radiation (ultra-relativistic matter with $p_r = \rho_r/3$), which satisfy the continuity equations $\hat{\nabla}_\mu T^{\mu\nu}_{(i)} = 0$ $(i = m, r)$, we can write the Friedmann equation (8) as

$$\left(\frac{H}{H_0}\right)^2 = \Omega_r a^{-4} + \Omega_{\rm m} a^{-3} + \Omega_k a^{-2} + \Omega_{\rm DE}(a). \tag{29}$$

Here, we define the canonical density parameters at the current epoch ($a_0 = 1$) as[8]

$$\Omega_{\rm m} \equiv \beta \frac{\rho_m^0}{3H_0^2},\ \Omega_r \equiv \beta \frac{\rho_r^0}{3H_0^2},\ \Omega_k \equiv -\gamma \frac{\mathcal{K}}{H_0^2 R_0^2},$$
$$\Omega_\Lambda \equiv \gamma \frac{\Lambda_W}{2H_0^2},\ \Omega_\omega \equiv \gamma \frac{\omega}{2H_0^2} \tag{30}$$

with positive parameters $\beta \equiv \kappa^2/2(3\lambda - 1)$, $\gamma \equiv \kappa^4 \mu^2 \Lambda_W / 8(3\lambda - 1)^2$, and introduce the (dynamical) dark-energy (HDE) component (Nilsson & Park 2022) as

$$\Omega_{\rm DE}(a) \equiv \left(\frac{\Omega_k^2}{4\Omega_\Lambda}\right) a^{-4} - \left(\frac{\Omega_k \Omega_\omega}{\Omega_\Lambda}\right) a^{-2} + \Omega_\Lambda, \tag{31}$$

which includes the *dark radiation* ($\sim a^{-4}$) and *dark curvature* ($\sim a^{-2}$) components as well as the cosmological constant component Ω_Λ. The Friedmann equation (29) is now given by

$$\left(\frac{H}{H_0}\right)^2 = \left(\Omega_r + \frac{\Omega_k^2}{4\Omega_\Lambda}\right) a^{-4} + \Omega_{\rm m} a^{-3} + \left(1 - \frac{\Omega_\omega}{\Omega_\Lambda}\right) \Omega_k a^{-2} + \Omega_\Lambda. \tag{32}$$

The EoS parameter (15) can be written as

$$w_{\rm DE}(a) = \frac{-12\,\Omega_\Lambda^2 a^4 + 4\Omega_k \Omega_\omega a^2 + \Omega_k^2}{12\,\Omega_\Lambda^2 a^4 - 12\Omega_k \Omega_\omega a^2 + 3\Omega_k^2}. \tag{33}$$

Then, from equation (28), the adiabatic sound speed can be obtained as

$$c_a^2 = \frac{\mathcal{K} + \bar{\omega} a^2}{3(\mathcal{K} - \bar{\omega} a^2)} = \frac{-2\Omega_\omega a^2 + \Omega_k}{6\Omega_\omega a^2 + 3\Omega_k}, \tag{34}$$

[8]We adopt the convention Ω_i for the current values and $\Omega_i(a)$ for the fully time-dependent values.

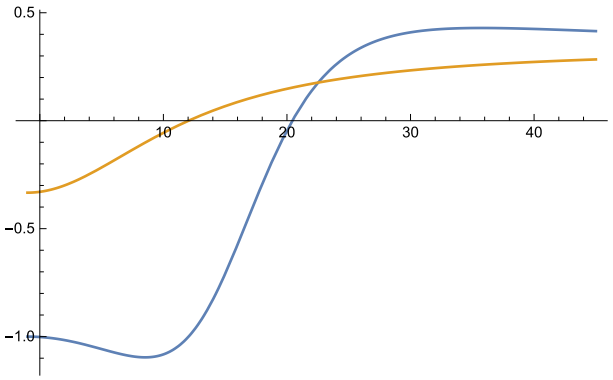

Figure 3. Plots of $w_{\rm DE}$ (blue), c_a^2 (yellow) versus $z = -1 + 1/a$ for our preferred case $\bar{\omega}\mathcal{K} < 0$ or $\Omega_\omega \Omega_k > 0$. Here, we take $\Omega_{\rm m} = 0.306$, $\Omega_r = 8.64 \times 10^{-5}$, $\Omega_k = -0.004$, $\Omega_\Lambda = 0.695$, $H_0 = 69.53$, $\Omega_\omega = -0.34$ from the previous background analysis, but with our preferred signature of $\Omega_\omega < 0$ (Nilsson & Park 2022).

which goes to $c_a^2 = 1/3$ in the UV limit (when $\mathcal{K} \neq 0$) and $c_a^2 = -1/3$ in the IR limit, but the evolution details depend on $\bar{\omega}$, $\mathcal{K}$ or Ω_ω, Ω_k (Fig. 2). It is interesting to note that the cosmological constant parts of $w_{\rm DE}$ in equation (33) do not contribute to c_a.

2.3 Comparison to Chevallier–Polarski–Linder (CPL) type parametrization

Our dark energy model described by $w_{\rm DE}$ (15) may have very rapid evolution or fluctuations with a phantom crossing at $w_{\rm DE} = -1$ as can be seen in Fig. 3. This might raise some questions on the relation of our dynamical dark energy model to the Chevallier–Polarski–Linder (CPL) type parametrization (Chevallier & Polarski 2001; Linder 2003),

$$w(a) = w_0 + w_a(1 - a) + w_b(1 - a)^2 + \cdots, \tag{35}$$

which is smoothly evolving but provides an excellent fit (at about 0.1 per cent level in observables).

To that end, we consider the comoving angular-diameter distance

$$d_A^c(z) = \frac{c}{H_0} \frac{1}{\sqrt{\Omega_k}} \,{\rm Sinh}\left[\sqrt{\Omega_k} \int_0^z \frac{{\rm d}z'}{H(z')/H_0}\right] \tag{36}$$

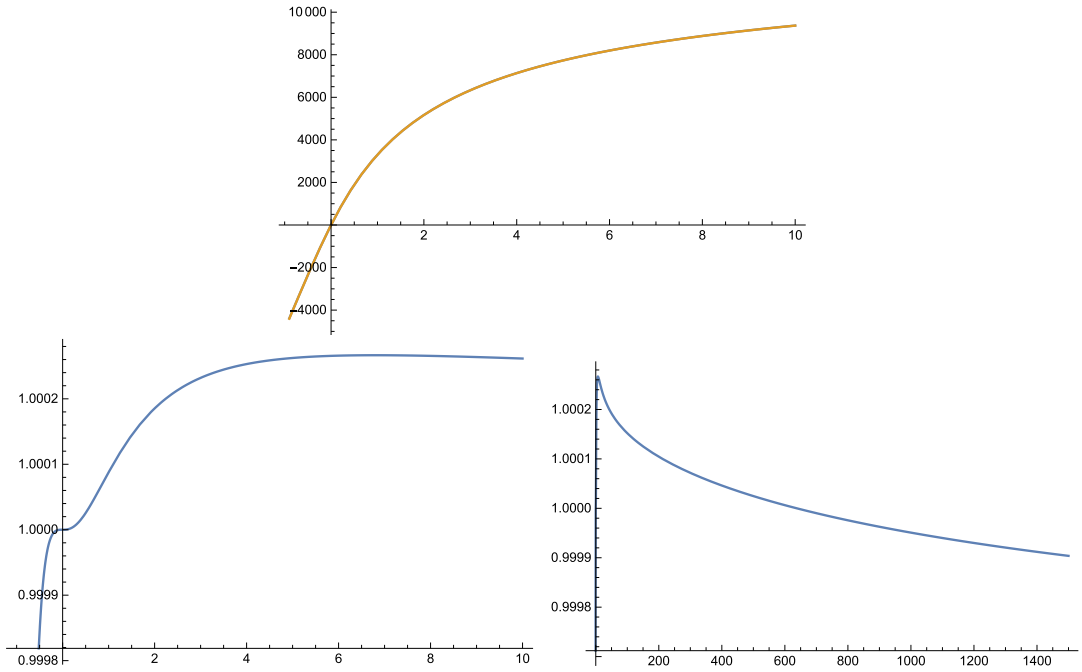

Figure 4. Comparison of the comoving angular-diameter distance $d_A^c(z)$ between our dark energy model for the preferred case in Fig. 3 and the corresponding CPL model with $w_0 = -1.002$, $w_a = -0.004$. The top plot shows the distances for the two cases with quite a good fit (the two curves are almost coincident). The bottom plots show the ratio of our preferred case versus the CPL model that provides the robustness of our dynamical dark energy model, even up to the CMB distance.

for the redshift $z = -1 + 1/a$. Here, the Hubble parameter $H(z)$ can be written as

$$\left(\frac{H(z)}{H_0}\right)^2 = \Omega_r(z+1)^4 + \Omega_m(z+1)^3 + \Omega_k(z+1)^2 + \Omega_{\rm DE}\cdot\exp\left(3\int_0^z \frac{1+w_{\rm DE}(z')}{1+z'}{\rm d}z'\right) \quad (37)$$

from the Friedmann equation (29) and the dark energy density parameter that solves the background conservation law (14),

$$\begin{aligned}\Omega_{\rm DE}(z) &= \Omega_{\rm DE}\cdot\exp\left[3\int_0^z \frac{1+w_{\rm DE}(z')}{1+z'}{\rm d}z'\right] \\ &= \Omega_{\rm DE}\cdot\exp\left[3(1+w_0+w_a)z(z+2) - \frac{3w_a z}{z+1} \right. \\ &\quad \left. + 3w_b\left(ln(z+1) - \frac{z(z+2)}{2(z+1)^2}\right) + \cdots\right] \end{aligned} \quad (38)$$

in the CPL-type parametrization (35). Now, in order to see the goodness of the *standard* CPL model with the first two parameters w_0, w_a, we compare the comoving angular-diameter distance (36) between our model with the full $w_{\rm DE}$ (15) and the CPL model with

$$\begin{aligned} w_0 &= \frac{-12\,\Omega_\Lambda^2 + 4\Omega_k\Omega_\omega + \Omega_k^2}{3\left(4\Omega_\Lambda^2 - 4\Omega_k\Omega_\omega + \Omega_k^2\right)}, \\ w_a &= \frac{16\,\Omega_k\left(4\Omega_\omega\Omega_\Lambda^2 - 4\Omega_k\Omega_\Lambda^2 + \Omega_k^2\Omega_\omega\right)}{3\left(4\Omega_\Lambda^2 - 4\Omega_k\Omega_\Lambda + \Omega_k^2\right)^2}, \end{aligned} \quad (39)$$

which can be obtained by expanding (15) near the current epoch $a = 1$. Our result in Fig. 4 shows that, even for the rapidly evolving case of dark energy in Fig. 3, the agreement is better than 0.03 per cent at all redshifts (0.006 per cent at the CMB distance $z \approx 1100$), which is sufficient for the current precision of data. From the fact that the comoving angular-diameter distance enters the CMB distance to the surface of last scattering, BAO, and SN observations, our result supports the robustness of our dynamical dark energy model (HDE) in comparison to the standard CPL model.[9]

2.4 Assumptions and initial conditions

We have introduced the dark energy fluid that is not interacting with other matter and radiation, by its purely gravitational origin. Their perturbation equations are very general and includes anisotropic stress σ, time-varying $w_{\rm DE}$, and arbitrary rest-frame sound speed $\hat{c}_s$. In the fluid approach, we have identified the background quantities $T^{\mu\nu}$ but have not specified other details about the perturbed quantities $\delta T^{\mu\nu}$, coming from the Lorentz-violating higher derivative terms in Hořava gravity. The only model dependence enters in the background $T^{\mu\nu}$ or the EoS parameter $w_{\rm DE}$ and all the other perturbation analysis can be very general, i.e. model independent. However, from equation (6), it might have its own limitation of validity by neglecting the genuine UV, i.e. deep subhorizon ($k \gg \mathcal{H}$), effects at the primordial universe: (6) assumes implicitly the same order of the second-order derivatives of gravitational perturbations $\delta G^{\mu\nu}$ as the fluid perturbations $\delta T^{\mu\nu}$, which contains the higher order derivatives of gravitational perturbations $\delta T^{\mu\nu}_{\rm DE}$ in addition to the conventional matter perturbations $\delta T^{\mu\nu}_{\rm matter}$ in our Hořava gravity model. Actually, equation (6) corresponds to a coarse-graining of the arbitrary perturbations and selects the spatially slowly varying and smooth gravity perturbations, while the background $T^{\mu\nu}$ may allow 'rapidly varying' $w_{\rm DE}$ due to the UV effect in a non-flat universe.

[9]This circumstance is quite similar to the vacuum metamorphosis (VM) model (Di Valentino, Linder & Melchiorri 2018, 2020b). In fact, even the asymptotic values of its EoS at UV and IR are the same and its rapidly evolving behaviour is quite similar. Understanding the physical relevance of the VM model to our dark energy model would be interesting.

Table 1. Flat priors adopted on the free parameters of the HDE model explored here.

Parameter	Prior
$\Omega_b h^2$	[0.005,0.1]
$\Omega_c h^2$	[0.001,0.99]
$100\theta_{\rm MC}$	[0.5,10]
τ	[0.01,0.8]
n_s	[0.8, 1.2]
$\log[10^{10}A_s]$	[1.61,3.91]
Ω_k	[−0.3, 0.3]
Ω_ω	[−100, 100]

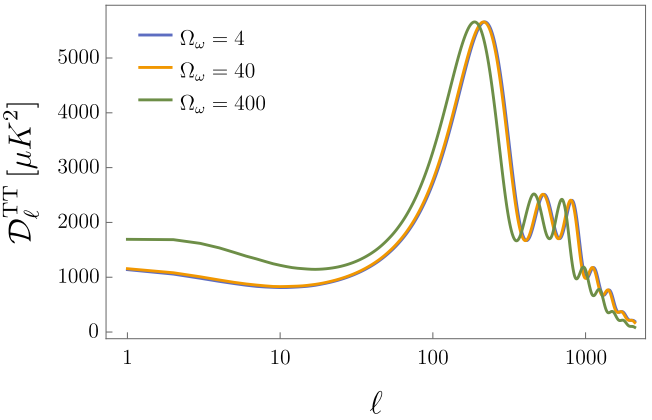

Figure 5. The CMB temperature power spectrum for different values of Ω_ω, while all the other parameters are fixed to a slightly closed universe with $\Omega_k = -0.001$. Given the symmetry for positive and negative values of Ω_ω and Ω_k that we discuss in the text, we show only positive Ω_ω. By increasing this parameter, we see a shift of the peaks towards lower multipoles, and an increase of the low-ℓ plateau.

The physical sound speed of dark-energy perturbations $\hat{c}_s$ can be arbitrary, but for the data analysis in the following sections, we will consider a *constant* $\hat{c}_s$ as a free parameter for simplicity; however, from the perturbation equations (26) and (27), $\hat{c}_s^2$ cannot be arbitrarily large for the stability of perturbations. Moreover, the anisotropic stress σ is an important parameter that characterizes the perturbations (Hu 1998) but constraining it seems to be difficult with the current precision (Yang et al. 2020). Therefore, we assume the absence of anisotropic stress σ in the following analysis.

For the initial conditions of dark energy perturbations in the early universe, i.e. during the radiation-dominated era where the perturbations are outside the (Hubble) horizon, we will consider the *adiabatic* initial perturbations of dark energy as (Koivisto & Mota 2006),

$$\delta_{\rm DE} = \left(\frac{1+w_\gamma}{1+w_{\rm DE}}\right)\delta_\gamma,\ \theta_{\rm DE} = \theta_\gamma, \tag{40}$$

where δ_γ, θ_γ are the initial perturbations of photons with $w_\gamma = 1/3$. Here, the velocity condition $\theta_{\rm DE} = \theta_\gamma$ is strictly valid for the adiabatic dark energy fluid, i.e. $\hat{c}_s^2 = c_a^2 = 1/3$, at UV. However, even for $\hat{c}_s^2 \neq c_a^2 = 1/3$, we will take the same initial condition in the following analysis since the late-time evolution is not (much) affected as far as $\hat{c}_s^2$ is inside some reasonable region (Koivisto & Mota 2006).

Finally, for the dynamical dark energy with a 'phantom crossing,' i.e. $w_{\rm DE} = -1$, the perturbation equation (27) looks divergent, i.e. unstable, for any non-vanishing $\hat{c}_s$. But it just means the vanishing density perturbation $\delta_{\rm DE} = 0$ at the instant and the equation (26) shows that later evolution may generate $\delta_{\rm DE}$ again for $w'_{\rm DE}\theta > 0$. In other words, the perturbation equations can be well-defined even at a phantom crossing.

3 METHODOLOGY AND DATA SETS

In this section, we list the current cosmological data sets used to constrain the HDE model:

(i) *Planck*: We make use of the full CMB temperature and polarization angular power spectra *plikTTTEEE+lowl+lowE* as released by Planck 2018 and used in Aghanim et al. (2020a,b).

(ii) *Lensing*: We consider the CMB lensing reconstruction likelihood from Planck 2018 (Aghanim et al. 2020c).

(iii) *BAO*: We add the BAO distance measurements from different astronomical surveys: 6dFGS (Beutler et al. 2011), SDSS-MGS (Ross et al. 2015), and BOSS DR12 (Alam et al. 2017).

Table 2. Parameter constraints at 68 per cent CL for an *open* universe on the independent (above the line) and dependent (below the line) parameters, together with the best-fitting χ^2 and its difference from the flat LCDM model.

Parameters	Planck	Planck +Lensing	Planck +BAO	Planck +Pantheon	Planck+Lensing +BAO+Pantheon
$\Omega_b h^2$	0.02255 ± 0.00017	0.02248 ± 0.00016	0.02239 ± 0.00015	0.02251 ± 0.00016	0.02240 ± 0.00015
$\Omega_c h^2$	0.1085 ± 0.0048	0.1155 ± 0.0034	0.1191 ± 0.0021	0.1105 ± 0.0044	0.1190 ± 0.0021
$100\theta_{\rm MC}$	1.04130 ± 0.00037	1.04112 ± 0.00034	1.04100 ± 0.00032	1.04124 ± 0.00034	1.04100 ± 0.00031
τ	0.0517 ± 0.0084	0.0517 ± 0.0081	0.0551 ± 0.0080	$0.0525^{+0.0081}_{-0.0073}$	0.0545 ± 0.0076
$\ln(10^{10}A_s)$	3.032 ± 0.018	3.034 ± 0.017	3.044 ± 0.016	3.035 ± 0.017	3.043 ± 0.015
n_s	0.9729 ± 0.0054	0.9696 ± 0.0050	0.9668 ± 0.0045	0.9716 ± 0.0051	0.9670 ± 0.0044
Ω_k	$0.00089^{+0.00029}_{-0.00034}$	$0.00056^{+0.00018}_{-0.00047}$	<0.000501	$0.00081^{+0.00029}_{-0.00037}$	<0.000464
Ω_ω	>56.1	40^{+20}_{-30}	23 ± 30	61^{+30}_{-20}	27^{+20}_{-30}
Ω_Λ	0.7146 ± 0.0077	0.7012 ± 0.0043	$0.6966^{+0.0023}_{-0.0026}$	0.7112 ± 0.0069	$0.6965^{+0.0021}_{-0.0023}$
$\Omega_{\rm m}$	0.2845 ± 0.0079	0.2983 ± 0.0044	$0.3030^{+0.0028}_{-0.0024}$	0.2880 ± 0.0071	$0.3031^{+0.0025}_{-0.0022}$
σ_8	$0.857^{+0.019}_{-0.014}$	0.823 ± 0.010	$0.820^{+0.012}_{-0.014}$	$0.852^{+0.018}_{-0.015}$	0.8189 ± 0.0092
S_8	0.834 ± 0.011	0.8210 ± 0.0090	0.824 ± 0.012	0.834 ± 0.011	0.8231 ± 0.0088
H_0 (km s^{-1} Mpc^{-1})	68.04 ± 0.44	68.18 ± 0.43	68.49 ± 0.39	68.13 ± 0.43	68.45 ± 0.36
$r_{\rm drag}$	147.29 ± 0.31	147.30 ± 0.32	147.13 ± 0.31	147.26 ± 0.31	147.15 ± 0.30
$\chi^2_{\rm bestfit}$	2755.4	2771.4	2770.5	3792.4	3815.4
$\Delta\chi^2_{\rm bestfit}$	−10.4	−3.2	−1.4	−8.7	−1.6

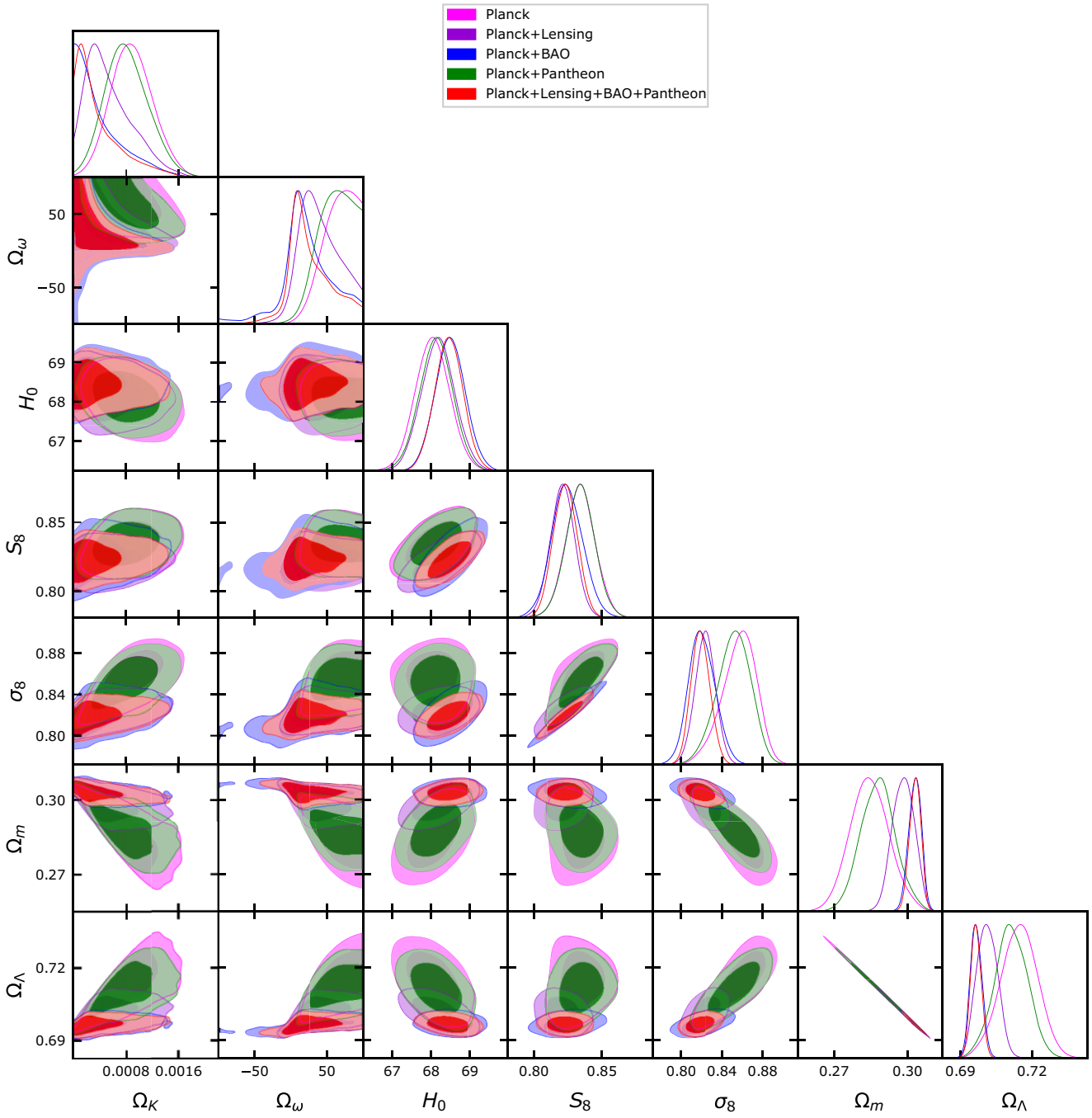

Figure 6. Triangular plot showing 2D contours at 68 per cent and 95 per cent CL and 1D posterior distributions of a few key parameters in an open HDE universe.

(iv) *Pantheon*: We include the Pantheon (Scolnic et al. 2018) sample of 1048 Type Ia SNe.

The parameter constraints are computed by means of MCMC sampling with our modified version of the publicly available packages CAMB (Lewis, Challinor & Lasenby 2000) and COSMOMC (Lewis & Bridle 2002).[10] The convergence diagnostic follows the Gelman and Rubin prescription (Gelman & Rubin 1992), which is already implemented in the Planck 2018 likelihood (Aghanim et al. 2020a).

In Table 1, we show the *flat* priors adopted in the data analysis. These are the physical density of baryons $\Omega_b h^2$, the physical density of CDM $\Omega_c h^2$, the ratio of sound horizon to the angular diameter distance at recombination $\theta_{\rm MC}$, the reionization optical depth τ, the scalar spectral index n_s, and the amplitude A_s of the primordial scalar power spectrum, the curvature of the universe Ω_k, and the HDE parameter Ω_ω. In particular, we analyse three cases: a closed universe where we restrict the Ω_k prior to $[-0.3, 0]$, an open universe with Ω_k in [0,0.3], and the full range listed in Table 1.

In Fig. 5, we show how variations in the HDE parameter Ω_ω affect the CMB temperature power spectrum, while all the other parameters are fixed to a slightly closed universe with $\Omega_k = -0.001$.

[10] http://cosmologist.info/cosmomc/

Table 3. Parameter constraints at 68 per cent CL for a *closed* universe on the independent (above the line) and dependent (below the line) parameters, together with the best-fitting χ^2 and its difference from the flat LCDM.

Parameters	Planck	Planck +Lensing	Planck +BAO	Planck +Pantheon	Planck+Lensing +BAO+Pantheon
$\Omega_b h^2$	0.02256 ± 0.00017	0.02248 ± 0.00016	0.02239 ± 0.00015	0.02253 ± 0.00017	0.02240 ± 0.00015
$\Omega_c h^2$	0.1091 ± 0.0047	0.1160 ± 0.0033	0.1195 ± 0.0021	0.1108 ± 0.0042	0.1194 ± 0.0021
$100\theta_{\rm MC}$	1.04132 ± 0.00037	1.04111 ± 0.00033	1.04101 ± 0.00032	1.04127 ± 0.00036	1.04100 ± 0.00031
τ	0.0520 ± 0.0080	0.0519 ± 0.0080	$0.0549^{+0.0072}_{-0.0081}$	0.0523 ± 0.0079	0.0546 ± 0.0075
$\ln(10^{10}A_s)$	3.032 ± 0.017	$3.034^{+0.018}_{-0.016}$	$3.044^{+0.015}_{-0.017}$	3.034 ± 0.017	3.043 ± 0.015
n_s	0.9729 ± 0.0054	0.9695 ± 0.0049	0.9721 ± 0.0053	0.9716 ± 0.0051	0.9669 ± 0.0044
Ω_k	$-0.00090^{+0.00034}_{-0.00029}$	$-0.00053^{+0.00046}_{-0.00016}$	>-0.000504	$-0.00083^{+0.00037}_{-0.00027}$	>-0.000471
Ω_ω	<-56.1	-41^{+34}_{-25}	-23 ± 34	-62^{+16}_{-33}	-22 ± 35
Ω_Λ	0.7150 ± 0.0078	$0.7011^{+0.0041}_{-0.0047}$	$0.6966^{+0.0023}_{-0.0026}$	0.7118 ± 0.0068	0.6964 ± 0.0023
$\Omega_{\rm m}$	0.2859 ± 0.0076	$0.2994^{+0.0045}_{-0.0040}$	$0.3038^{+0.0025}_{-0.0022}$	0.2891 ± 0.0066	0.3040 ± 0.0022
σ_8	$0.858^{+0.018}_{-0.014}$	0.8232 ± 0.0098	$0.820^{+0.012}_{-0.014}$	$0.852^{+0.018}_{-0.014}$	0.8184 ± 0.0094
S_8	0.837 ± 0.011	0.8223 ± 0.0092	0.826 ± 0.012	0.836 ± 0.011	0.8239 ± 0.0090
H_0 (km s^{-1} Mpc^{-1})	68.02 ± 0.44	68.17 ± 0.43	68.49 ± 0.38	68.09 ± 0.44	68.46 ± 0.37
$r_{\rm drag}$	147.29 ± 0.31	147.31 ± 0.31	147.13 ± 0.30	147.27 ± 0.31	147.15 ± 0.29
$\chi^2_{\rm bestfit}$	2755.6	2771.5	2770.5	3792.5	3815.4
$\Delta\chi^2_{\rm bestfit}$	-10.4	-3.2	-1.4	-8.6	-1.6

We can see that by increasing the value of Ω_ω we obtain a shift of the peaks towards lower multipoles, and an increase of the low-ℓ plateau.

4 RESULTS

In this section, we present the results we obtained for the HDE model in the three different cases: an open universe in Table 2 and Fig. 6, a closed universe in Table 3 and Fig. 7, and the full range for positive and negative values of the curvature in Table 4 and Fig. 8. For completeness, we test in Appendix A what happens with a $\hat{c}_s^2$ free to vary as an additional parameter. Moreover, for comparison, we include similar Tables A2 and A3 with the same data sets combination for the flat and non-flat LCDM models, respectively, in Appendix B. In each table, we present the constraints on the cosmological parameters at 68 per cent confidence level (CL), and in the last two rows, we report the best fit, i.e. minimum, χ^2 and its difference from the flat LCDM model as described above. Our noticeable results are as follows:

(i) Regarding Ω_k in Tables 2 and 3, we see, for Planck alone or Planck+Pantheon, a preference for an open (closed) universe at more than 95 per cent CL (see also Figs 6 and 7). However, when we include the lensing likelihood we see that the preference for an open (closed) universe is about just 1σ. Moreover, when we add the BAO data, the lower bound of Ω_k is constrained to be close to zero and it can be consistent with a flat universe. We also note that the constraints on Ω_k are not Gaussian. The preference for a non-flat universe for Planck alone is similar to the standard non-flat LCDM (see Table A3 in Appendix B). But, contrary to the preference of a *closed* universe in the LCDM scenario (Aghanim et al. 2020b; Di Valentino et al. 2019, 2021f; Handley 2021; Yang et al. 2022; Semenaite et al. 2022), the two separate cases with positive and negative curvature are almost symmetric and moreover, as we can notice from the best-fitting χ^2, they are equally probable so that there is no preference of one case over the other. This will be the reason why the full case shown in Table 4 gives for the Ω_k the average of the two separate cases, preferring therefore an almost null value $\Omega_k \approx 0$, which gives back the flat LCDM, with an accumulated uncertainty which is very small but enough to nullify the average value, though even better with BAO.

(ii) Ω_ω is a newly introduced parameter in our model with no *a priori* known constraints (cf. Nilsson & Park 2022). Our results show an intimate relation of $\Omega_\omega \propto \Omega_k$ and the properties for Ω_k still apply to Ω_ω also, e.g. for Planck alone or Planck+Pantheon, a preference for $\Omega_\omega > 0$ ($\Omega_\omega < 0$) in an open (closed) universe, while Ω_ω is more poorly constrained than Ω_k. Actually, one can easily notice that 2D contours for the cut of $\Omega_\omega > 0$ in Fig. 6 (or $\Omega_\omega < 0$ in Fig. 7) can be mapped on to the corresponding 2D contours for Ω_k, while the other contours for $\Omega_\omega < 0$ (or $\Omega_\omega > 0$) rapidly decays to zero[11] and are believed to be numerical errors. This property will explain the similarities between 2D contours involving Ω_k and Ω_ω for the full Ω_k case shown in Fig. 8. Moreover, within our results alone, there is no preference of $\Omega_\omega < 0$ over $\Omega_\omega > 0$ or vice versa, just as for Ω_k. This is the reason why we find Ω_ω unconstrained for Planck and Planck+Pantheon data, while it is constrained to be close to zero for all the remaining data set combinations. However, if we choose $\Omega_\omega < 0$ from astrophysical arguments – the absence of a *complex* metric inside a black hole with a positive cosmological constant $\Lambda > 0$ (Argüelles et al. 2015),[12] the above relation $\Omega_\omega \propto \Omega_k$ makes us choose a closed universe, i.e. $\Omega_k < 0$, consistently with our preferred result in the earlier work (Nilsson & Park 2022).

(iii) Regarding the cosmic tensions involving the Hubble constant H_0 and cosmic shear parameter S_8, we obtain a positive result because we can break the correlation between them: we have a shift of H_0 towards a higher value by 1σ, though not enough to solve the Hubble constant tension, leaving the value of the cosmic shear S_8 unaltered (see for comparison the flat and non-flat LCDM cases in Tables A2 and A3). This is in contrast to the exacerbated tension for a non-flat LCDM, where $H_0 = 54.4^{+3.3}_{-4.0}$ km s^{-1} Mpc^{-1}, $S_8 = 0.981 \pm 0.049$ (see Table A3) for Planck alone, with a decreasing H_0

[11] A similar behaviour for Ω_k is expected if the positive and negative values of Ω_ω are considered separately.

[12] The required condition may be written as $\Omega_\omega(\Omega_\omega - 2\Omega_\Lambda) > 0$ (Argüelles et al. 2015). If we rule out the possibility of $\Omega_\omega > 0$, $\Omega_\omega > 2\Omega_\Lambda$ in our case (see Fig. 6), we have only the choice of $\Omega_\omega < 0$ from $\Omega_\Lambda > 0$.

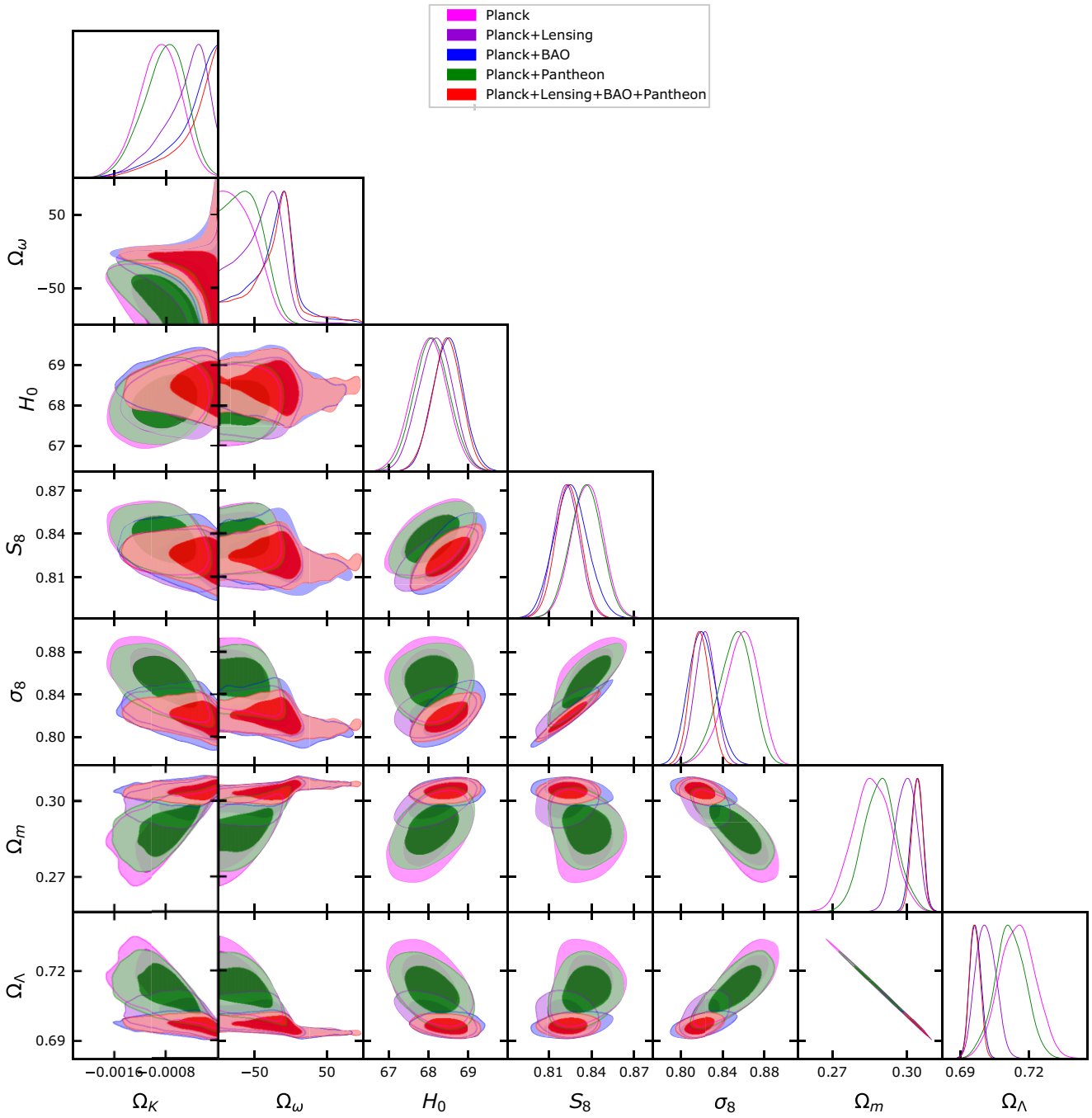

Figure 7. Triangular plot showing 2D contours at 68 per cent and 95 per cent CL and 1D posterior distributions of a few key parameters in a closed HDE universe.

but increasing S_8, as well as other models for improving H_0 (Knox & Millea 2020; Jedamzik et al. 2021; Di Valentino et al. 2021a; Perivolaropoulos & Skara 2022), because in the HDE case we do not see the noticeable correlation between Ω_k and H_0 (or S_8) (see Figs 6 and 7) that is present in the non-flat LCDM case. Moreover, our results for different data sets show that S_8 has a shift towards a lower value, in agreement with the non-flat LCDM case, when we add the BAO in the data set combinations, while H_0 has a 1σ shift towards a higher value. However, we can see the usual positive correlation between H_0 and S_8 in each data set, so that S_8 is increased as H_0 is increased. On the other hand, as we can notice in our results (Tables 2–4), this behaviour does not depend on the curvature.

(iv) For all other parameters, there are some significant shifts, especially the matter density $\Omega_{\rm m}$ and the dark energy density Ω_Λ with respect to a flat LCDM for all data set combinations. However, our results are more similar to the conventional value $\Omega_{\rm m} \sim 0.3$ and $\Omega_\Lambda \sim 0.7$, contrary to the standard non-flat LCDM result that shows $\Omega_m \sim 0.5$ and $\Omega_\Lambda \sim 0.5$ for Planck alone (Aghanim et al. 2020b; Di Valentino et al. 2019, 2021f; Handley 2021; Yang et al. 2022). For the other parameters, like $\Omega_b h^2$, $\Omega_c h^2$, $\theta_{\rm MC}$, τ, A_s, n_s, and $r_{\rm drag}$ that are not shown in Figs 6–8, there are a few shifts

Table 4. Parameter constraints at 68 per cent CL for a full Ω_k universe on the independent (above the line) and dependent (below the line) parameters, together with the best-fitting χ^2 and its difference from the flat LCDM.

Parameters	Planck	Planck +Lensing	Planck +BAO	Planck +Pantheon	Planck+Lensing +BAO+Pantheon
$\Omega_b h^2$	0.02254 ± 0.00017	0.02248 ± 0.00016	0.02239 ± 0.00015	0.02254 ± 0.00017	0.02241 ± 0.00015
$\Omega_c h^2$	0.1092 ± 0.0048	0.1157 ± 0.0033	0.1193 ± 0.0022	0.1104 ± 0.0043	0.1191 ± 0.0022
$100\theta_{\rm MC}$	1.04130 ± 0.00036	1.04112 ± 0.00033	1.04100 ± 0.00032	1.04125 ± 0.00035	1.04100 ± 0.00031
τ	0.0522 ± 0.0077	0.0517 ± 0.0080	0.0552 ± 0.0080	0.0530 ± 0.0079	0.0548 ± 0.0074
$\ln(10^{10} A_s)$	3.033 ± 0.018	3.034 ± 0.017	3.044 ± 0.017	3.035 ± 0.017	3.043 ± 0.015
n_s	0.9727 ± 0.0053	0.9698 ± 0.0050	0.9668 ± 0.0046	0.9723 ± 0.0051	0.9670 ± 0.0044
Ω_k	0.00000 ± 0.00095	-0.00001 ± 0.00068	-0.00001 ± 0.00054	-0.00002 ± 0.00090	-0.00001 ± 0.00053
Ω_ω	Unconstrained	-1 ± 48	-2 ± 43	Unconstrained	-2 ± 42
Ω_Λ	0.7143 ± 0.0078	0.7013 ± 0.0043	$0.6966^{+0.0023}_{-0.0027}$	0.7118 ± 0.0068	$0.6965^{+0.0020}_{-0.0023}$
$\Omega_{\rm m}$	0.2857 ± 0.0079	0.2987 ± 0.0043	$0.3034^{+0.0028}_{-0.0023}$	0.2882 ± 0.0068	$0.3035^{+0.0024}_{-0.0022}$
σ_8	$0.857^{+0.019}_{-0.015}$	0.824 ± 0.010	$0.821^{+0.012}_{-0.014}$	$0.852^{+0.018}_{-0.014}$	0.8185 ± 0.0092
S_8	0.836 ± 0.011	0.8218 ± 0.0090	0.825 ± 0.012	0.835 ± 0.011	0.8232 ± 0.0088
H_0 (km s^{-1} Mpc^{-1})	68.06 ± 0.44	68.17 ± 0.42	68.49 ± 0.39	68.07 ± 0.43	68.43 ± 0.37
$r_{\rm drag}$	147.28 ± 0.31	147.31 ± 0.31	147.12 ± 0.30	147.28 ± 0.30	147.17 ± 0.29
$\chi^2_{\rm bestfit}$	2755.6	2771.5	2770.5	3792.7	3815.4
$\Delta\chi^2_{\rm bestfit}$	-10.2	-3.1	-1.4	-8.4	-1.6

for Planck, Planck+Pantheon, or Planck+Lensing, but once BAO data are included and the parameter degeneracies are broken, the HDE values are very similar to the LCDM ones. This may give a positive indication for our HDE model against a non-flat LCDM, even though there are no important improvements in the best-fitting χ^2 (see Table A3), but there are against the LCDM case, as shown in the difference of the best-fitting χ^2 from the flat LCDM (see Tables 2–4). An exception is the Planck+Pantheon case, where HDE performs significantly better than both LCDM and non-flat LCDM. Hence, even if our model is assuming curvature in the universe, the results are close to *cosmic concordance*, i.e. consistency with different cosmic observations (see Figs 6, 7, and 9) and they do not depend on the curvature.

5 CONCLUDING REMARKS

In conclusion, we have tested the *perturbed* dynamical dark energy model in Hořava gravity (HDE) due to an *effective* energy–momentum tensor from the extra Lorentz-violating terms. By treating the dark energy perturbations over the background perfect fluid HDE as general fluid perturbations, we perform the full CMB data analysis via CAMB/COSMOMC as well as BAO and supernovae (SNe) Ia data. Except for the BAO case, we have obtained the preference for a *non-flat* universe, though the sign of the curvature parameter is not determined unless we use additional arguments. Thus, regarding the curvature parameter Ω_k, BAO is not consistent with other observations and this could indicate some *flat* biases of BAO data points used in our analysis (Glanville, Howlett & Davis 2022). On the other hand, we obtain some positive results that seem to indicate that we are in the right direction towards a resolution of cosmic tensions. First, we obtained a positive result on the internal cosmic tension between the Hubble constant H_0 and cosmic shear parameter S_8, since we have a shift of H_0 towards a higher value by 1σ, though not enough for resolving H_0 tension, but the value of the cosmic shear S_8 is unaltered. This is in contrast to a decreasing H_0 but increasing S_8 in non-flat LCDM (Aghanim et al. 2020b; Di Valentino et al. 2019; 2021d, f; Handley 2021). Secondly, for all other parameters, we obtain comparable results to those of LCDM especially with BAO, e.g. $\Omega_{\rm m} \sim 0.3$ and $\Omega_\Lambda \sim 0.7$, so that our results are close to a *cosmic concordance*, contrary to a recent non-flat LCDM result. However, our results show also some undesirable features compared to our previous background analysis with the CMB distance priors (Nilsson & Park 2022), like less improvement of the H_0 tension itself, degeneracy between $(\bar{\omega}, \mathcal{K}) \leftrightarrow (-\bar{\omega}, -\mathcal{K})$, and the resulting almost *null* results on $\bar{\omega}, \mathcal{K}$ or equivalently Ω_ω, Ω_k if we do not restrict to $\mathcal{K} \neq 0$. Several promising directions for improving our analysis are as follows:

(i) The degeneracy between $(\bar{\omega}, \mathcal{K}) \leftrightarrow (-\bar{\omega}, -\mathcal{K})$ is the characteristic feature of $\Omega_{\rm DE}$ for the Hořava cosmology background and there are some remnants in our previous background analysis (model B) as well (Nilsson & Park 2022), though not quite as strong as in the current analysis. However, in another HDE model (model A), which has a parameter $\Delta N_{\rm eff}$ representing a possible excess in the standard effective number of relativistic species $N_{\rm eff} = 3.044$, the degeneracy is removed and we have obtained (a) non-null results on Ω_ω, Ω_k with the preference of a closed universe and (b) a more improved H_0 tension. So, extending our present analysis with $\Delta N_{\rm eff}$ as in the dark energy model A (Nilsson & Park 2022) and/or varying $N_{\rm eff}$ can be a promising way to improve our results.

(ii) There is still no direct observational evidence for the interaction between dark matter and dark energy. However, it seems that a hypothetical dark energy model with the interaction, which is called the 'interacting dark energy (IDE) model' may provide another appealing solution to H_0 and S_8 tensions (Di Valentino et al. 2020a, 2021e). Actually, in our Hořava gravity set-up, the interaction could be natural if we can introduce CDM from the gravity sector also, as proposed in footnote 2. So, extending our analysis with the phenomenological interaction parameter for dark matter and energy, even without knowing the detailed mechanism, can also be an interesting way to improve our results.

(iii) In the cosmological perturbation around the spatially flat FLRW background, the leading scale-invariant spectrum for the scalar mode depends on the combination of UV parameters $\widetilde{\alpha}_4 \equiv \alpha_4 + 2\alpha_5/3 + 8\alpha_6/3$, which vanishes for the parameters from the DBC (equation 5). So, we need to relax the DBC for UV parameters to obtain a scale-invariant *scalar* power spectrum and the result would be still valid in a non-flat universe since the non-flatness just gives

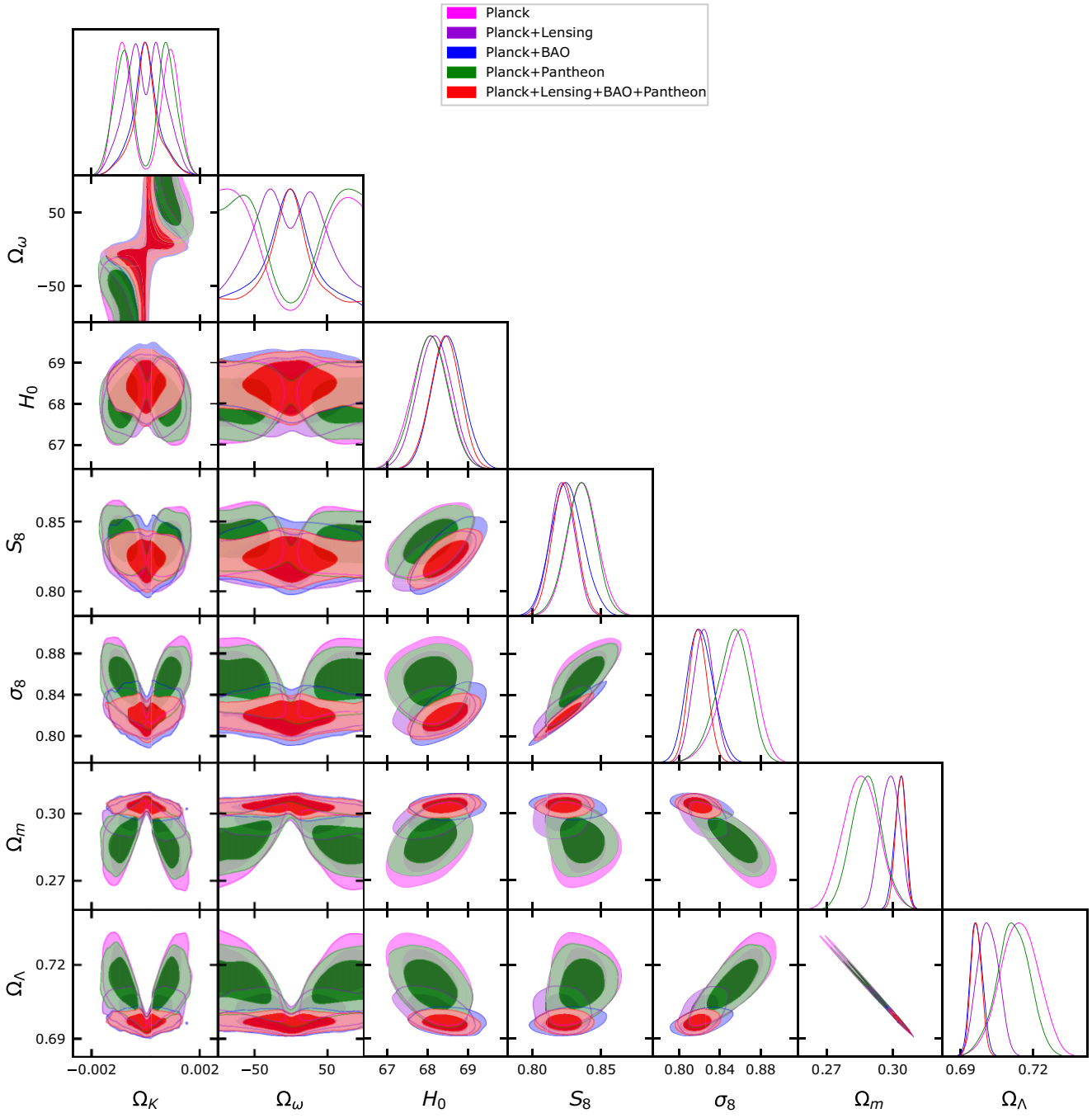

Figure 8. Triangular plot showing 2D contours at 68 per cent and 95 per cent CL and 1D posterior distributions of a few key parameters in the full Ω_k universe.

some subleading corrections to the flat cosmology perturbations. However, our result from CAMB/COSMOMC shows an almost scale-invariant *matter* power spectrum as usual and does not seem to depend much on the choice of UV parameters. This seems to be an evidence that we have lost some of the genuine UV effects in the dark energy perturbations from the coarse graining in our fluid approach. The undesirable features in our result might be due to this problem as well.

So, considering the full perturbation analysis for a non-flat universe with the corresponding modifications in the CAMB code would be a challenging way for the improvement. Phenomenologically, it seems that the general analysis may correspond to relaxing a vanishing anisotropic stress condition $\sigma = 0$, since this condition would be due to some peculiar way of cancellation of arbitrary perturbations that would be anisotropic generally. So, considering a non-vanishing anisotropic stress condition (Hu 1998) can also be an interesting way for the improvement within the current fluid approach.

(iv) In this paper, we considered $\lambda = 1$ for simplicity of our analysis. If we consider an arbitrary $\lambda \neq 1$, as we noted in footnote 5, the fundamental constants defined in the Einstein equation (6) and the Friedmann equations (8) and (9) are different and we need to consider the effective speed of light, Newton's constant, and cosmological constant $c_{\rm eff}^2 = (8(3\lambda-1)^2)^{-1}\kappa^4\mu^2\Lambda_W$, $G_{\rm eff} = (16\pi(3\lambda-1))^{-1}\kappa^2 c_{\rm eff}^2$, and $\Lambda_{\rm eff} = (3/2)\Lambda_W c_{\rm eff}^2$, respectively. All the coupling

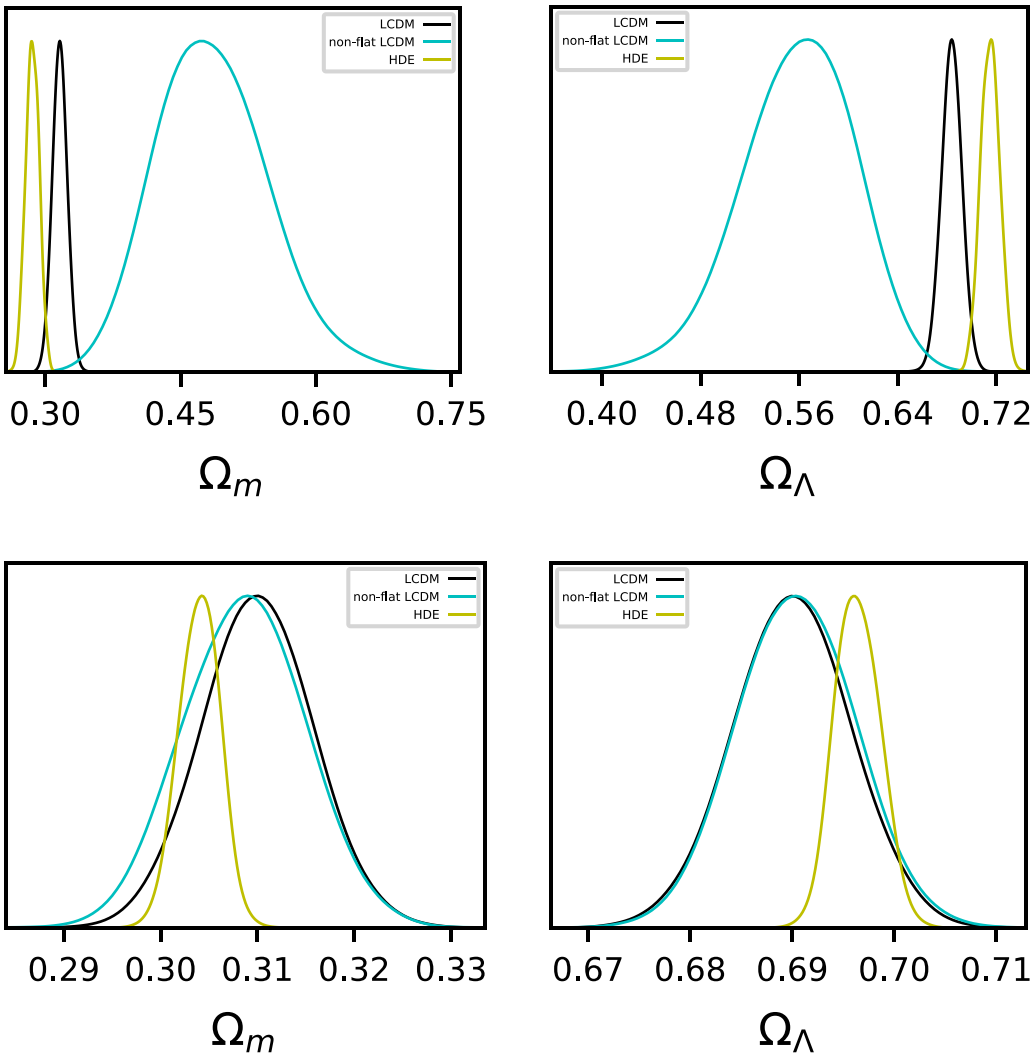

Figure 9. 1D posteriors on Ω_m and Ω_Λ for a closed universe scenario in our HDE model versus the flat and non-flat LCDM models for Planck (top panels), Planck+Lensing+BAO+Pantheon (bottom panels). 2D contour on Ω_m versus Ω_Λ is almost a line from $\Omega_\Lambda \approx 1 - \Omega_m$ (see Figs 6, 7, and 9).

constants λ, κ, μ, and Λ_W could flow under renormalization group (RG) so that the fundamental constants could also flow in the cosmic evolution. The fully consistent treatment of these evolving constants is beyond the scope of this paper, but one might estimate the amount of RG flow from the existing cosmic tensions. For example, if we assume $c_{\rm eff} = c$ and $\Lambda_{\rm eff} = \Lambda$ as the current values and they do not RG run but only λ can run, then one can find $G_{\rm eff} = 2(3\lambda - 1)^{-1}G$, where $G = (32\pi G)^{-1}\kappa^2 c_{\rm eff}^2$ is the Newton's constant in the Einstein equations (6) even for arbitrary λ and it coincides with the Newton's constant in the Friedmann equations (8) and (9) for $\lambda = 1$ (Dutta & Saridakis 2010; Frusciante et al. 2016; Frusciante & Benetti 2021). In this simple example, G either runs or does not run depending on the running behaviours of κ and μ: (i) if $\kappa =$ fixed and $\mu^2/(3\lambda - 1)^2 =$ fixed, we have $G =$ fixed and $G_{\rm eff} \sim (3\lambda - 1)^{-1}$, or (ii) if $\mu =$ fixed and $\kappa^4/(3\lambda - 1)^2 =$ fixed, we have $G_{\rm eff} =$ fixed and $G \sim (3\lambda - 1)^{-1}$; if we choose G as the current value and do not run as in case (i), $G_{\rm eff}$ shows the *asymptotically free* behaviour at $\lambda = 1/3$, which is thought to be a UV fixed point (Barvinsky, Herrero-Valea & Sibiryakov 2019), whereas if we choose $G_{\rm eff}$ as the current value and do not run as in case (ii), G shows the asymptotically free behaviour. If we consider the spatially flat case $\mathcal{K} = 0$, and neglect the small cosmological constant term by considering the early universe, one can find that the Hubble parameter $H(t)_{\lambda \neq 1}$ has an additional factor compared to the Hubble parameter for $\lambda = 1$ as $H(t)_{\lambda \neq 1} \approx 2(3\lambda - 1)^{-1}H(t)_{\lambda = 1}$. If we consider the RG flow of $\lambda_{\rm IR} = 1 \to \lambda_{\rm UV} = 0.9$, we can obtain about 10 per cent increase of the Hubble parameter $H(t)_{\lambda \neq 1}$ compared to what is expected for $\lambda = 1$, $H(t)_{\lambda = 1}$ (see also Nilsson 2020). In other words, the Hubble tension might be an indication of RG flow on λ. Moreover, we would expect that all the (fundamental) perturbation equations, like the evolution equations for matter density contrast, are also governed by the effective constant $G_{\rm eff}$ as in the background Friedmann equations so that S_8 could be also affected. It would be interesting to see the effect of $\lambda \neq 1$ in the cosmic tensions with the full data set analysis and observe the indication of RG flows in our cosmic evolution.

ACKNOWLEDGEMENTS

EDV is supported by a Royal Society Dorothy Hodgkin Research Fellowship. NAN and MIP were supported by Basic Science Research Program through the National Research Foundation of Korea (NRF) funded by the Ministry of Education, Science and Technology (2020R1A2C1010372 to NAN; 2020R1A2C1010372 and

2020R1A6A1A03047877 to MIP). This article is based upon work from COST Action CA21136 addressing observational tensions in cosmology with systematics and fundamental physics (CosmoVerse) supported by COST (European Cooperation in Science and Technology). We acknowledge IT Services at The University of Sheffield for the provision of services for High Performance Computing.

DATA AVAILABILITY

The data sets used in this work to constrain the models are public data available in their respective references.

REFERENCES

Abbott T. M. C. et al., 2022a, preprint (arXiv:2207.05766)
Abbott T. M. C. et al., 2022b, Phys. Rev. D, 105, 023520
Abdalla E. et al., 2022, J. High Energy Astrophys., 34, 49
Aghanim N. et al., 2020a, A&A, 641, A5
Aghanim N. et al., 2020b, A&A, 641, A6
Aghanim N. et al., 2020c, A&A, 641, A8
Alam S. et al., 2017, MNRAS, 470, 2617
Argüelles C., Grandi N., Park M.-I., 2015, J. High Energy Phys., 10, 100
Arnowitt R. L., Deser S., Misner C. W., 2008, Gen. Relativ. Grav., 40, 1997
Asgari M. et al., 2021, A&A, 645, A104
Bardeen J. M., 1980, Phys. Rev. D, 22, 1882
Barvinsky A. O., Herrero-Valea M., Sibiryakov S. M., 2019, Phys. Rev. D, 100, 026012
Bellorin J., Restuccia A., 2011, Phys. Rev. D, 84, 104037
Beutler F. et al., 2011, MNRAS, 416, 3017
Blas D., Pujolas O., Sibiryakov S., 2009, J. High Energy Phys., 10, 029
Blas D., Pujolas O., Sibiryakov S., 2010, Phys. Rev. Lett., 104, 181302
Bogdanos C., Saridakis E. N., 2010, Class. Quantum Gravity, 27, 075005
Cerioni A., Brandenberger R. H., 2011, JCAP, 08, 015
Chevallier M., Polarski D., 2001, Int. J. Mod. Phys. D, 10, 213
Devecioglu D. O., Park M.-I., 2021, preprint (arXiv:2112.00576)
DeWitt B. S., 1967, Phys. Rev., 160, 1113
Di Valentino E., Linder E. V., Melchiorri A., 2018, Phys. Rev. D, 97, 043528
Di Valentino E., Melchiorri A., Silk J., 2019, Nature Astron., 4, 196
Di Valentino E., Melchiorri A., Mena O., Vagnozzi S., 2020a, Phys. Dark Univ., 30, 100666
Di Valentino E., Linder E. V., Melchiorri A., 2020b, Phys. Dark Univ., 30, 100733
Di Valentino E. et al., 2021a, Class. Quantum Gravity, 38, 153001
Di Valentino E. et al., 2021b, Astropart. Phys., 131, 102604
Di Valentino E. et al., 2021c, Astropart. Phys., 131, 102605
Di Valentino E. et al., 2021d, Astropart. Phys., 131, 102607
Di Valentino E., Melchiorri A., Mena O., Pan S., Yang W., 2021e, MNRAS, 502, L23
Di Valentino E., Melchiorri A., Silk J., 2021f, ApJ, 908, L9
Dutta S., Saridakis E. N., 2010, JCAP, 05, 013
Friedman A., 1922, Z. Phys., 10, 377
Frusciante N., Benetti M., 2021, Phys. Rev. D, 103, 104060
Frusciante N., Raveri M., Vernieri D., Hu B., Silvestri A., 2016, Phys. Dark Univ., 13, 7
Gao X., Wang Y., Brandenberger R., Riotto A., 2010, Phys. Rev. D, 81, 083508
Gavela M. B., Hernandez D., Lopez Honorez L., Mena O., Rigolin S., 2009, JCAP, 07, 034
Gelman A., Rubin D. B., 1992, Statist. Sci., 7, 457
Glanville A., Howlett C., Davis T. M., 2022, MNRAS, 517, 3087
Handley W., 2021, Phys. Rev. D, 103, L041301
Horava P., 2009, Phys. Rev. D, 79, 084008
Hu W., 1998, ApJ, 506, 485
Hu W., Seljak U., White M. J., Zaldarriaga M., 1998, Phys. Rev. D, 57, 3290
Jacobson T., Mattingly D., 2004, Phys. Rev. D, 70, 024003
Jedamzik K., Pogosian L., Zhao G.-B., 2021, Commun. Phys., 4, 123
Kamionkowski M., Riess A. G., 2022, preprint (arXiv:2211.04492)
Kehagias A., Sfetsos K., 2009, Phys. Lett. B, 678, 123
Knox L., Millea M., 2020, Phys. Rev. D, 101, 043533
Kodama H., Sasaki M., 1984, Prog. Theor. Phys. Suppl., 78, 1
Koivisto T., Mota D. F., 2006, Phys. Rev. D, 73, 083502
Koyama K., Arroja F., 2010, J. High Energy Phys., 03, 061
Lemaitre G., 1927, Ann. Soc. Sci. Bruxelles A, 47, 49
Lewis A., Bridle S., 2002, Phys. Rev. D, 66, 103511
Lewis A., Challinor A., Lasenby A., 2000, ApJ, 538, 473
Lifshitz E., 1941, Zh. Eksp. Teor. Fiz., 11, 255 & 269
Linder E. V., 2003, Phys. Rev. Lett., 90, 091301
Ma C.-P., Bertschinger E., 1995, ApJ, 455, 7
Mukohyama S., 2009, Phys. Rev. D, 80, 064005
Nilsson N. A., 2020, Eur. Phys. J. Plus, 135, 361
Nilsson N. A., Park M.-I., 2022, Eur. Phys. J. C, 82, 873
O'Neal-Ault K., Bailey Q. G., Nilsson N. A., 2021, Phys. Rev. D, 103, 044010
Park M.-i., 2011, Class. Quantum Gravity, 28, 015004
Park M.-I., 2009, J. High Energy Phys., 09, 123
Perivolaropoulos L., Skara F., 2022, New Astron. Rev., 95, 101659
Peter P., Uzan J.-P., 2013, Primordial Cosmology. Oxford Univ. Press, Oxford
Riess A. G. et al., 2022, ApJ, 934, L7
Robert C. P., 2015, preprint (arXiv:1504.01896)
Ross A. J., Samushia L., Howlett C., Percival W. J., Burden A., Manera M., 2015, MNRAS, 449, 835
Ryden B., 1970, Introduction to Cosmology. Cambridge Univ. Press, Cambridge
Scolnic D. M. et al., 2018, ApJ, 859, 101
Semenaite A. et al., 2022, preprint (arXiv:2210.07304)
Shah P., Lemos P., Lahav O., 2021, A&AR, 29, 9
Shin S., Park M.-I., 2017, JCAP, 12, 033
Verde L., Treu T., Riess A. G., 2019, Nature Astron., 3, 891
Vilenkin N. Y., Smorodinskii Y. A., 1964, Sov. Phys. JETP, 19, 1209
Wang A., 2017, Int. J. Mod. Phys. D, 26, 1730014
Yang W., Pan S., Mota D. F., Du M., 2020, MNRAS, 497, 879
Yang W., Giarè W., Pan S., Di Valentino E., Melchiorri A., Silk J., 2022, preprint (arXiv:2210.09865)

APPENDIX A: TESTING THE HDE MODEL WITH A VARYING $\hat{c}_s^2$

In this appendix, we test the HDE model with a varying $\hat{c}_s^2$ in the range $[-10,10]$ as an additional parameter and we report the results in Table A1 and Fig. A1. As we can see, this additional parameter is completely unconstrained and uncorrelated from the other parameters of the model, making the canonical choice of $\hat{c}_s^2 = 1$ in our main data analysis justifiable (Tables A2 and A3).

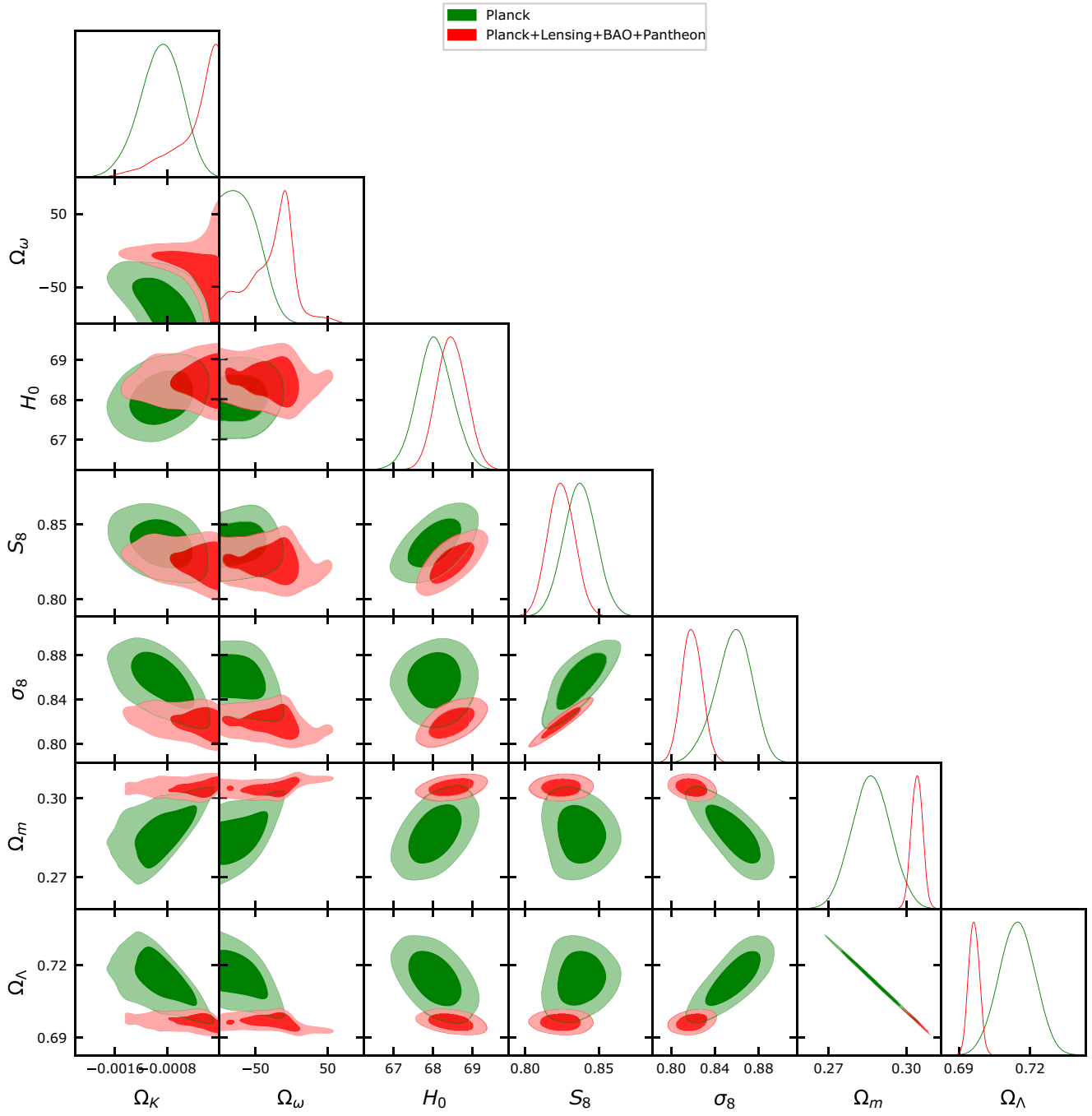

Figure A1. Triangular plot showing 2D contours at 68 per cent and 95 per cent CL and 1D posterior distributions of a few key parameters for a closed universe, once $\hat{c}_s^2$ is free to vary in the range $[-10,10]$.

Table A1. Parameter constraints at 68 per cent CL for a closed universe, once $\hat{c}_s^2$ is free to vary in the range [−10,10], on the independent (above the line) and dependent (below the line) parameters, together with the best-fitting χ^2.

Parameters	Planck	Planck+Lensing +BAO+Pantheon
$\Omega_b h^2$	0.02255 ± 0.00017	0.02239 ± 0.00015
$\Omega_c h^2$	0.1094 ± 0.0046	0.1195 ± 0.0022
$100\theta_{\rm MC}$	$1.04130^{+0.00034}_{-0.00039}$	1.04099 ± 0.00032
τ	0.0519 ± 0.0080	0.0548 ± 0.0077
$\ln(10^{10}A_s)$	3.032 ± 0.011	3.043 ± 0.015
n_s	0.9729 ± 0.0055	0.9670 ± 0.0044
Ω_k	$-0.00090^{+0.00035}_{-0.00029}$	>-0.00047
Ω_ω	<-55.0	-27^{+33}_{-24}
$\hat{c}_s^2$	unconstrained	unconstrained
Ω_Λ	0.7145 ± 0.0075	0.6964 ± 0.0022
$\Omega_{\rm m}$	0.2864 ± 0.0074	0.3040 ± 0.0022
σ_8	$0.857^{+0.018}_{-0.015}$	0.8190 ± 0.0092
S_8	0.837 ± 0.011	0.8244 ± 0.0090
H_0 (km s^{-1} Mpc^{-1})	68.04 ± 0.45	68.47 ± 0.37
$r_{\rm drag}$	147.28 ± 0.31	147.15 ± 0.29
$\chi^2_{\rm best\,fit}$	2755.4	3815.3

APPENDIX B: COMPARISON OF THE FLAT AND NON-FLAT LCDM MODELS

In this appendix, we report for comparison the constraints on the cosmological parameters for the flat and non-flat LCDM models in Tables A2 and A3 for the same data set combinations explored in this work.

This paper has been typeset from a TEX/LATEX file prepared by the author.

Table A2. Parameter constraints at 68 per cent CL for a flat LCDM universe.

Parameters	Planck	Planck +Lensing	Planck +BAO	Planck +Pantheon	Planck+Lensing +BAO+Pantheon
$\Omega_b h^2$	0.02236 ± 0.00015	0.02237 ± 0.00015	0.02242 ± 0.00014	0.02239 ± 0.00014	0.02243 ± 0.00013
$\Omega_c h^2$	0.1202 ± 0.0014	0.1200 ± 0.0012	0.11933 ± 0.00091	0.1199 ± 0.0013	0.11921 ± 0.00089
$100\theta_{\rm MC}$	1.04090 ± 0.00031	1.04092 ± 0.00031	1.04101 ± 0.00029	1.04094 ± 0.00031	1.04102 ± 0.00029
τ	0.0546 ± 0.0078	0.0544 ± 0.0073	0.0561 ± 0.0071	0.0550 ± 0.0078	0.0564 ± 0.0071
$\ln(10^{10}A_s)$	3.045 ± 0.016	3.044 ± 0.014	3.047 ± 0.014	3.046 ± 0.016	3.047 ± 0.014
n_s	0.9648 ± 0.0043	0.9649 ± 0.0042	0.9665 ± 0.0038	0.9655 ± 0.0042	0.9668 ± 0.0037
Ω_Λ	0.6834 ± 0.0085	0.6847 ± 0.0073	0.6889 ± 0.0056	0.6855 ± 0.0079	0.6897 ± 0.0054
$\Omega_{\rm m}$	0.3166 ± 0.0085	0.3153 ± 0.0073	0.3111 ± 0.0056	0.3145 ± 0.0079	0.3103 ± 0.0054
σ_8	0.8122 ± 0.0073	0.832 ± 0.013	0.8102 ± 0.0060	0.8114 ± 0.0074	0.8100 ± 0.0060
S_8	0.834 ± 0.016	0.832 ± 0.013	0.825 ± 0.011	0.831 ± 0.015	0.824 ± 0.010
H_0 (km s^{-1} Mpc^{-1})	67.27 ± 0.61	67.36 ± 0.54	67.66 ± 0.42	67.42 ± 0.57	67.72 ± 0.40
$r_{\rm drag}$	147.05 ± 0.30	147.09 ± 0.26	147.21 ± 0.23	147.11 ± 0.29	147.23 ± 0.23
$\chi^2_{\rm best\,fit}$	2765.8	2774.6	2771.9	3801.1	3817.0

Table A3. Parameter constraints at 68 per cent CL for a non-flat LCDM universe, together with the best-fitting χ^2 and its difference from the flat LCDM.

Parameters	Planck	Planck +Lensing	Planck +BAO	Planck +Pantheon	Planck + Lensing +BAO + Pantheon
$\Omega_b h^2$	0.02260 ± 0.00017	0.02249 ± 0.00016	0.02239 ± 0.00015	0.02247 ± 0.00017	0.02240 ± 0.00015
$\Omega_c h^2$	0.1181 ± 0.0015	0.1185 ± 0.0015	0.1197 ± 0.0014	0.1190 ± 0.0015	0.1196 ± 0.0014
$100\theta_{\rm MC}$	1.04116 ± 0.00033	1.04107 ± 0.00032	1.04095 ± 0.00031	1.04102 ± 0.00033	1.04096 ± 0.00032
τ	0.0486 ± 0.0082	$0.0497^{+0.0082}_{-0.0071}$	0.0548 ± 0.0078	0.0548 ± 0.0077	0.0559 ± 0.0073
$\ln(10^{10}A_s)$	3.028 ± 0.017	$3.030^{+0.017}_{-0.015}$	3.044 ± 0.016	3.043 ± 0.016	3.047 ± 0.014
n_s	0.9706 ± 0.0048	0.9688 ± 0.0047	0.9659 ± 0.0045	0.9677 ± 0.0047	$0.9661^{+0.0042}_{-0.0047}$
Ω_k	$-0.044^{+0.018}_{-0.015}$	-0.0106 ± 0.0065	0.0008 ± 0.0019	$-0.0064^{+0.0061}_{-0.0054}$	0.0008 ± 0.0019
Ω_Λ	$0.560^{+0.050}_{-0.043}$	0.659 ± 0.017	0.6894 ± 0.0061	0.670 ± 0.017	0.6901 ± 0.0059
$\Omega_{\rm m}$	$0.485^{+0.058}_{-0.068}$	0.352 ± 0.023	0.3098 ± 0.0066	0.337 ± 0.022	0.3087 ± 0.0056
σ_8	0.774 ± 0.015	0.795 ± 0.011	0.8109 ± 0.0084	0.8044 ± 0.0096	0.8115 ± 0.0072
S_8	0.981 ± 0.049	0.860 ± 0.021	0.824 ± 0.013	0.852 ± 0.025	0.824 ± 0.010
H_0 (km s^{-1} Mpc^{-1})	$54.4^{+3.3}_{-4.0}$	$63.6^{+2.1}_{-2.3}$	67.88 ± 0.68	65.1 ± 2.2	67.94 ± 0.64
$r_{\rm drag}$	147.35 ± 0.30	147.36 ± 0.31	147.15 ± 0.31	147.25 ± 0.31	147.16 ± 0.29
$\chi^2_{\rm best\,fit}$	2754.5	2771.4	2771.4	3799.3	3816.9
$\Delta\chi^2_{\rm best\,fit}$	−11.3	−3.2	−0.5	−1.8	−0.1